Multiple Coulomb Scattering in MicroBooNE

David Kaleko*[1], Leonidas Kalousis[2], Polina Abratenko[3], Mike Shaevitz[1], Josh Spitz[3], and [AUTHOR LIST FOR THIS NOTE SHOWN, ANYTHING PUBLIC WILL BE COLLABORATION-WIDE][4]

[1]Columbia University, NY
[2]Vrije Universiteit Brussel, Belgium
[3]University of Michigan, MI
[4]Misc

December 19, 2016

Abstract

Liquid Argon Time Projection Chambers (LArTPCs) are an important detector technology for the future of the neutrino physics community. This technology provides precise three-dimensional reconstruction of charged particle tracks that traverse the detector medium. The MicroBooNE experiment is a LArTPC at the Fermi National Accelerator laboratory with active volume dimensions of 2.6 m width $\times$ 2.3 m height $\times$ 10.4 m length located in the Booster Neutrino Beamline (BNB) which has a peak neutrino energy of about 0.7 GeV. In this note, we discuss a technique of measuring a charged particle's momentum by means of Multiple Coulomb Scattering (MCS), which does not require the full track to be contained inside of the detector volume as other track momentum reconstruction methods do (range-based momentum reconstruction and calorimetric momentum reconstruction). In this note we provide motivation for why this technique is important, demonstrate and quantify its performance on fully contained neutrino-induced muon tracks both in simulation and in data. In general we find good agreement between data and simulation, with small bias in the momentum reconstruction and with resolutions that vary as a function of track length, decreasing from about 12% for the shortest (one meter long) tracks when scattering deviations over 10 centimeter segments are used in the MCS algorithm. This technote also describes other uses for multiple coulomb scattering besides momentum reconstruction, including identification of poorly reconstructed tracks, determination of track direction, and particle identification.

*Corresponding Author

Contents

1 Note Message and Content Overview **4**

2 Introduction and Motivation **5**

3 MCS Implementation Using the Maximum Likelihood Method **7**
3.1 Track Segmentation . . . 7
3.2 Scattering Angle Computation . . . 8
3.3 Maximum Likelihood Theory . . . 8
3.4 Maximum Likelihood Implementation . . . 9

4 MCS Performance on Truth-Selected Muons from numuCC Events in Simulation **11**
4.1 Input Sample . . . 11
4.2 Fiducial Volume Definition . . . 11
4.3 Performance with MCTracks . . . 11
4.3.1 MCTrack Description . . . 11
4.3.2 Event Selection . . . 12
4.3.3 Range Energy Validation . . . 13
4.3.4 MCS Momentum Validation . . . 14
4.3.5 Highland Validation . . . 17
4.4 Performance with Reconstructed Tracks . . . 17
4.4.1 Event Selection . . . 17
4.4.2 MCS Momentum Validation . . . 18
4.4.3 Highland Validation . . . 20

5 MCS Performance on Automatically Selected Muons from numuCC Events With Cosmics in Simulation **21**
5.1 Input Sample . . . 21
5.2 Event Selection . . . 21
5.3 MCS Momentum Validation . . . 22
5.4 Highland Validation . . . 22

6 MCS Performance on Automatically Selected Muons from numuCC Events in MicroBooNE Data **26**
6.1 Input Sample . . . 26
6.2 Event Selection . . . 26
6.3 MCS Momentum Validation . . . 27
6.4 Highland Validation . . . 28

7 Conclusions and Outlook **32**

8 Possible Plots for Publication **34**

Appendix A Optimizing Segment Length **37**

Appendix B Optimizing Constant Detector Resolution Term **37**

64 **Appendix C MCS to Determine Track Direction** **39**

65 **Appendix D Inverse Momentum to Quantify Resolution: Justification** **40**

66 **Appendix E Track Angle Dependence** **42**

1 Note Message and Content Overview

This is a technote internal to the MicroBooNE collaboration quantifying the performance of the Multiple Coulomb Scattering (MCS) based momentum estimation technique. The message of this note is that MCS is an important technique for LArTPCs measuring neutrino interactions, and we have demonstrated the MCS technique works and we have quantified its performance both on simulation and data. This note is a demonstration of performance but is not an end-all inclusive study on the algorithm and subsequently has limited scope. At the end of this note are some suggestions for future analyses which have not been done yet. *The message of this note is simply "MicroBooNE has demonstrated that it's likelihood-based MCS method for measuring muon momenta works specifically on contained tracks from BNB neutrinos. We describe how the method works, and we quantify how well it works."*

Ideally this analysis will lead to a publication in a journal like JINST, which will also have a limited scope. A list of potential plots to be included in the publication can be found at the end of this note, in Section 8.

In general the structure of this note is as follows:

1. An introduction to the MicroBooNE detector, and motivation for the MCS method for this experiment and within the future LArTPC community.
2. A detailed description of how the actual method works.
3. Demonstration of this method on a high-statistics sample of truth-selected muons from simulated numu charged-current interactions. This sample is relevant because the muons have the momentum and angle spectra that one would expect in MicroBooNE from the BNB. MCS performance is demonstrated both for MCTracks in this sample, and well-reconstructed pandoraNuPMA tracks.
   - The purpose of demonstrating that the technique works with MCTracks (which come from true GEANT4 energy depositions in the detector) is to serve as a "best-case" baseline before reconstruction effects are convolved.
   - The purpose of demonstrating that this technique works with automatically reconstructed tracks is to get one step closer towards a data/MC comparison.

   This input sample is also used in additional studies including optimizing the segment length used in the algorithm, optimizing the additional constant resolution term used in the algorithm, studying the algorithm performance as a function of track angle, as well as a potential additional use for the technique: determining track directionality. These studies can be found in the appendices.
4. Demonstration of this method on automatically-selected well-reconstructed neutrino events in the full MicroBooNE BNB + cosmics simulation. The purpose of this section is to take another step towards working with real automatically-selected BNB data. This section describes particle misidentification (MID) rates, MCS PID capabilities, and other things that the previous (truth-based selection) section does not.
5. Demonstration of this method on automatically-selected real neutrino events in actual MicroBooNE BNB data. In order to ensure the tracks are well-reconstructed and to mitigate MIDs, a handscanning effort is used and is described in this section.
6. A conclusion section reiterating the usefulness of the tool, describing the outlook of the algorithm and potential additional studies that could be done, along with a list of plots that might be good to put in a potential publication derived from this note.

2 Introduction and Motivation

MicroBooNE (Micro Booster Neutrino Experiment) is an experiment based at the Fermi National Accelerator Laboratory (Fermilab) that uses a large Liquid Argon Time Projection Chamber (LArTPC) to investigate the excess of low energy events observed by the MiniBooNE experiment [1] and to study neutrino-argon cross-sections. MicroBooNE is part of the Short-Baseline Neutrino (SBN) physics program, along with two other LArTPCs: the Short Baseline Near Detector (SBND) and the Imaging Cosmic And Rare Underground Signal (ICARUS) detector. MicroBooNE also provides important research and development in terms of detector technology and event reconstruction techniques for future LArTPC experiments including DUNE (Deep Underground Neutrino Experiment).

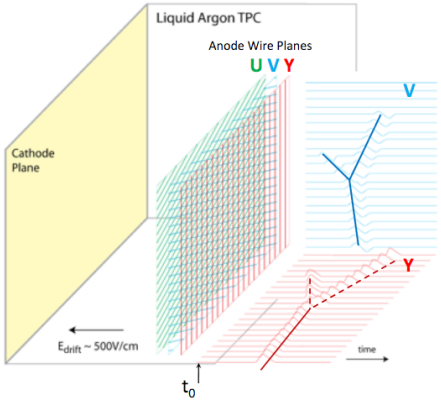

Figure 1: *A diagram of the time projection chamber of the MicroBooNE detector [2].*

The MicroBooNE detector is currently the largest LArTPC in the United States. It consists of a rectangular time projection chamber (TPC) with dimensions 2.6 m width $\times$ 2.3 m height $\times$ 10.4 m length located 470 m away from the Booster Neutrino Beam (BNB) target. Time projection chambers, filled with a gas or liquid volume, are used to analyze particle interactions in three dimensions. The x-direction of the TPC corresponds to the drift coordinate, the y-direction is the vertical direction, and the z-direction is the direction along the beam. The amount of active liquid argon in the TPC is 89 tons, with the total cryostat containing 170 tons of liquid argon. Liquid argon is chosen to fill the volume for a variety of reasons: argon contains a high density of nucleons, which allows for a greater rate of interactions with particles within the medium; argon ionizes easily; it is transparent to its own scintillation light; it has a high electron lifetime; and it is inexpensive.

Photomultiplier tubes (PMTs) and three wire planes with 3mm spacing at angles of 0, and $\pm$ 60 degrees with respect to the vertical are located in the TPC to aid with event reconstruction (Figure 1). In a neutrino interaction, a neutrino from the beam interacts with the argon and the charged outgoing child particles traverse the medium, losing energy and leaving an ionization trail. The resulting electrons drift to the anode side of the TPC, containing the wire planes, away from the negatively charged cathode plate on the opposite side. The movement of electrons induces a current in the wires, which is used

to create three distinct two-dimensional views of the event. Combining these wire signals with timing information from the PMTs allows for full three-dimensional reconstruction of the event.

The BNB is predominantly composed of muon neutrinos, which can undergo charge-current interactions in the TPC and produce muons. For muon tracks that are completely contained in the TPC, it is straightforward to calculate the momentum with a measurement of the length of the particle's track. Around half of muons from BNB neutrino events in MicroBooNE are not fully contained in the TPC, and therefore using length-based calculations for these uncontained tracks is not a possibility. The only way to compute the energy of an outgoing three-dimensional track is by means of multiple coulomb scattering (MCS).

The phenomenon of multiple coulomb scattering (MCS) occurs when a charged particle enters a medium and undergoes electromagnetic scattering with the atomic nuclei. This scattering deviates the original trajectory of the particle within the material (Figure 2). For a given energy, the scatters of a track-like particle (in terms of angular deflection relative to the track direction) form a gaussian distribution centered at zero with a standard deviation given by the Highland-Lynch-Dahl formula [3][4] (henceforth referred to as the Highland formula):

$$\sigma_o = \frac{13.6 \text{ MeV}}{p\beta c} z \sqrt{\frac{\ell}{X_0}} \Big[1 + 0.0038 \ln\Big(\frac{\ell}{X_0}\Big)\Big] \tag{1}$$

where β is the ratio of the particle's velocity to the speed of light, ℓ is the distance traveled inside the material, z is the magnitude of the charge of the particle, and X_0 is the radiation length of the target material (taken to be a constant 14 cm in liquid argon). With the Highland formula, the momentum of a track-like particle can be determined using only the 3D reconstructed track it produces in the detector, without any calorimetric information. The method by which this is done is described in detail in Section 3. Within neutrino physics, past emulsion detectors like the DONUT [5] and OPERA [6] experiments have used MCS to determine particle momenta. Additionally, the MACRO [7] experiment at Gran Sasso Laboratory utilized this technique as well. The original method for using MCS to determine particle momentum in a LArTPC involved using a Kalman Filter and was originally described by the ICARUS collaboration [8], and the likelihood-based method described in this technote for use in the MicroBooNE detector was originally described by Leonidas Kalousis [9].

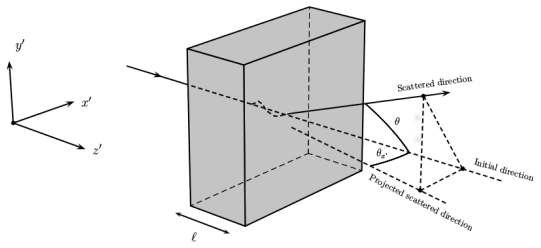

Figure 2: *The particle's trajectory is deflected as it traverses through the material [9].*

3 MCS Implementation Using the Maximum Likelihood Method

This section describes exactly how the phenomenon of multiple coulomb scattering is leveraged to determine the momentum of a track-like particle reconstructed in a LArTPC. In general, the approach is as follows:

1. The three-dimensional track is broken up into segments of configurable length.
2. The scattering angles between consecutive segments are measured.
3. Those angles combined with the Highland formula (Equation 2) are used to build a likelihood that the particle has a specific momentum, taking into account energy loss in upstream segments of the track.
4. The momentum corresponding to the maximum likelihood is chosen to be the MCS computed momentum.

Each of these steps are discussed in detail in the following subsections.

The idea and initial implementation of MCS using the maximum likelihood method for this analysis is credited to Leonidas Kalousis, a former member of the MicroBooNE collaboration. Further details regarding the technique can be found in his internal notes concerning both Monte Carlo simulated tracks [9] and reconstructed tracks [10]. Only slight modifications to this code have been made for the analysis described in this note (for example removing the relativistic approximation, and a bug fix in which only scatters in the x' direction were used in the likelihood [Section 3.2]).

For this analysis, a minimum start-to-end reconstructed track length of 100 cm was used. A minimum length is required to allow for sufficient scatters to measure the momentum. With 100 cm tracks and 10 cm segments (see Section 3.1), eighteen scattering measurements, coming from nine pairs of segments times two measurements (one in each of the x' and y' directions) per pair, will ultimately be used to reconstruct the momentum of the particle (see Section 3.2).

3.1 Track Segmentation

The input to the track segmentation routine is a vector of ordered three-dimensional trajectory points (x,y,z) representing the reconstructed track. The points are ordered along the direction of the track, with the first point representing the start of the track, and the last point representing the end of the track. These trajectory points can be determined in a number of ways by different track reconstruction algorithms. In the case of this analysis, the track reconstruction algorithm is named "pandoraNuPMA" which constructs these three-dimensional trajectory points by combining two-dimensional hits reconstructed from signals on the different wire planes along with timing information from the photomultiplier tubes to reconstruct the third dimension [11]. Note that the tracking resolution in the y- (vertical) and z- (beam) directions are determined by the wire plane spacings, while the resolution in the x- (drift) direction is determined by optical signal timing and therefore the x- direction resolution is better than that of the y- and z- directions.

Also input to the track segmentation routine is the desired segment length, which is a tunable parameter. In this note, segment lengths are always taken to be 10 cm (based on the findings of Appendix

A) except where otherwise explicitly stated. This routine begins at the start of the track, and iterates through the trajectory points in order, each time computing the straight-line distance between the first point and the current one. When a point is reached that is greater than the desired segment length, that iteration stops and the direction cosines of this segment are computed.

Given the subset of the three-dimensional trajectory points (x, y, z) that correspond to one "segment" of the track, a three-dimensional linear fit is applied to the data points using the orthogonal distance regression method around the trajectory point averages for that segment. This method finds the eigenvalues and eigenvectors of the (data - average) covariance matrix and the solution is the one associated with the maximum eigenvalue. All trajectory points have equal weight in the fit. There is no goodness-of-fit requirement. It is worth noting that delta rays can deposit energy locally and somewhat off the muon trajectory, resulting in shifted trajectory points. The MCS algorithm does not attempt to remove delta rays or correct for this in any way; it assumes the reconstructed track does not include trajectory points corresponding to energy deposited by delta rays.

At the end of this routine, a vector of length n (where n is the number of segments for the track) is stored containing the direction cosines at the start of each segment.

3.2 Scattering Angle Computation

This routine within the MCS code takes as input the vector of length n (where n is the number of segments for the track) containing the direction cosines at the start of each segment. In general, the algorithm iterates over consecutive pairs of segments (the segmentation routine is described in Section 3.1) and computes angular scatters between each, and stores them for later use by a future subroutine. This code is more complicated than just taking the dot product between consecutive direction cosines to find the total angular scatter between segments because the Highland formula is derived from scattering independently in the two directions orthogonal to the direction of the track. For this reason, this subroutine performs a coordinate transformation for each pair of segments such that the direction of first of the two segments is along the z' direction, as drawn in Figure 2. With the z' direction defined as such, x' and y' directions are chosen such that all of x', y', and z' are mutually orthogonal, again shown in Figure 2[1]. The scattering angles both in the x' and y' planes are then computed for each consecutive pairs of segments[2]. After this routine, a vector of length $2n$ is stored containing the scattering angles in the x' plane as well as in the y' plane. These scattering angles are what are input into the maximum likelihood routine to determine track momentum.

3.3 Maximum Likelihood Theory

The normal probability distribution for a variable with a gaussian error sigma is given by:

$$f_X(\Delta\theta) = (2\pi\sigma_o^2)^{-\frac{1}{2}} exp(-\frac{1}{2}\frac{(\Delta\theta - \mu_o)^2}{\sigma_o^2}) \quad (2)$$

[1]Note that at this point, all of x', y', and z' are different than the detector coordinates, x, y, and z which correspond to drift direction, vertical direction, and beam direction respectively.

[2]Both of these scattering angles are used downstream in the MCS algorithm, and therefore the choice of x' and y' are not important.

Here, each $\Delta\theta$ corresponds to a scattering angle measurement between one pair of segments in a track either in the rotated-coordinates x' or y' plane (both are used in the algorithm), μ_o is assumed to be zero, and σ_o is the RMS angular deflection computed by the modified Highland formula (Equation 6), which is a function of both the momentum and the length of that segment. Since energy is lost between segments, σ_o is different for each angular measurement along the track so we replace σ_o with $\sigma_{o,j}$, where j is an index representative of the segment.

To get the likelihood, one takes the product of $f_X(\Delta\theta_j)$ over all the $\Delta\theta_j$ segment-to-segment scatters along the track. Since the product of exponentials is just an exponential with the sum of the arguments, this product becomes

$$L(\mu_o;(\sigma_{o,1})^2,...,(\sigma_{o,n})^2;\Delta\theta_1,...,\Delta\theta_n)=\prod_{j=1}^{n}f_X(\Delta\theta_j,\mu_o,(\sigma_{o,j})^2)=(2\pi)^{\frac{-n}{2}}\times\prod_{j=1}^{n}(\sigma_{o,j})^{-1}\times exp(-\frac{1}{2}\sum_{j=1}^{n}\frac{(\Delta\theta_j-\mu_o)^2}{(\sigma_{o,j})^2}) \tag{3}$$

In practice, rather than maximizing likelihood it is often more computationally convenient to instead minimize the negative log likelihood. Taking the natural logarithm of the likelihood L gives an expression that is related to a χ^2

$$l(\mu_o;(\sigma_{o,1})^2,...,(\sigma_{o,n})^2;\Delta\theta_1,...,\Delta\theta_n)=ln(L)=-\frac{n}{2}ln(2\pi)-\sum_{j=1}^{n}ln(\sigma_{o,j})-\frac{1}{2}\sum_{j=1}^{n}\frac{(\Delta\theta_j-\mu_o)^2}{(\sigma_{o,j})^2} \tag{4}$$

The negative log likelihood for one specific segment's angular scatter $\Delta\theta_j$ given an expected scattering RMS $\sigma_{o,j}$ is given by the following equation

$$-l(\mu_o,\sigma_{o,j},\Delta\theta_j)=\frac{1}{2}ln(2\pi)+ln(\sigma_{o,j})+\frac{1}{2}\frac{(\Delta\theta_j-\mu_o)^2}{(\sigma_{o,j})^2} \tag{5}$$

In general, Equation 5 is evaluated for each segment in a track given a postulated full track momentum, and the sum of these terms is used to determine the likelihood that the postulated track momentum is correct for that track.

3.4 Maximum Likelihood Implementation

Given a set of angular deflections in the x' and y' planes for each segment as described in Section 3.2, a modified version of the Highland formula (Equation 6) is used along with a maximum likelihood method to determine the momentum of the track.

$$\sigma_o^{RMS}=\sqrt{(\sigma_o)^2+(\sigma_o^{res})^2}=\sqrt{(\frac{13.6\text{ MeV}}{p\beta c}z\sqrt{\frac{\ell}{X_0}}\Big[1+0.0038\ln\Big(\frac{\ell}{X_0}\Big)\Big])^2+(\sigma_o^{res})^2} \tag{6}$$

where the formula is "modified" from the original Highland formula (Equation 2) in that it includes a detector-inherent angular resolution term σ_o^{res} which is given a fixed value of 2 mrad in all studies contained in this note as described in Appendix B[10]. Note that the author of this note uses the term "modified Highland formula" to correspond to Equation 6, but outside of this technote this terminology may be used to refer to Lynch and Dahl's modifications to Highland's *original* formula. The original formula is not shown [3], but Lynch and Dahl's modifications are Equation 2 [4].

In general, this routine does a raster scan over postulated track energies in steps of 1 MeV from a minimum of 1 MeV up to a maximum of 7.5 GeV. Ending at 7.5 GeV as a maximum momentum is valid because given the BNB spectrum, no neutrino-induced tracks above that momentum are expected in MicroBooNE[3].

Given a postulated full track momentum, p_t, the full track energy E_t is computed from the usual energy momentum relation,

$$E_t^2 = p_t^2 + m_\mu^2 \tag{7}$$

where p_t is the full track momentum and m_μ is the mass of the muon. The maximum likelihood algorithm iterates over angular scatters for each segment, with two $\Delta\theta_j$ values for each segment (corresponding to the x' and y' scattering planes). The energy of the jth segment is given by

$$E_j = E_t - k_{cal} * N_{upstream} * l_{seg} \tag{8}$$

where k_{cal} is the minimally ionizing energy constant given to be $2.105\frac{MeV}{cm}$ in liquid argon[12][4], $N_{upstream}$ is the number of segments upstream of this particular segment, and l_{seg} is the segmentation length[5]. This definition of E_j therefore takes into account energy loss along the track, and can be negative for steps in the raster scan. In the case a segment energy E_j is negative, this step in the raster scan is skipped (this will happen for any step in the raster scan in which the postulated energy of the track E_t is less than $k_{cal} * N_{segments} * l_{seg}$). The value of segment energy, E_j is used to predict the RMS angular scatter for that segment (σ_o^{RMS}) by way of a modified version of Highland formula, Equation 6. Still assuming the mean angular scatter, μ_o, is zero, Equation 5 is evaluated for each segment and all evaluations are summed to compute a total summed negative log likelihood for that postulated track energy, E_t.

After the raster scan over postulated track momenta is complete, the one with the smallest summed negative log likelihood is chosen to be the final MCS computed momentum for the track.

[3]Note that 7.5 GeV might not be sufficiently high for muons from NUMI beam neutrinos, but that is outside the scope of this analysis which is geared specifically towards BNB neutrinos

[4]k_{cal} is the minimum ionization energy lost by muons and in general stopping muons are not minimally ionizing close to their stopping point.

[5]Note that measuring the energy loss directly via calorimetric methods is likely a more appropriate way to compute E_j (especially since one can potentially then incorporate energy lost to delta rays) but incorporating calorimetry is outside the scope of this analysis

4 MCS Performance on Truth-Selected Muons from numuCC Events in Simulation

In this section, studies from this truth-selected simulated BNB numuCC muon sample with MCTracks are described. Additionally, similar studies on this sample using automatically reconstructed tracks is described. This section also includes a study justifying that range-based energy is an accurate predictor of true energy for contained muons (with bias less than 1% and resolution better than 4%), and therefore can be used in place of true energy so as to compare MC directly to data. The MCS performance on this sample of MCTracks is shown to be comparable to that on automatically reconstructed PandoraNuPMA tracks when the track is well reconstructed, with a bias below 5% and a resolution that varies between 2 and 10%, performing better for higher momentum (longer) tracks. The resolution is slightly worse for reconstructed tracks than for MCtracks. Additionally, the scattering angle of track segments for a given momentum is shown to be similarly gaussian both for MCTracks and well reconstructed tracks, in line with the Highland formula prediction.

4.1 Input Sample

The input sample to this portion of the analysis is is 772,000 MCC7 simulated BNB neutrino interactions without any cosmics simulated. These simulated events are run through a fully automated reconstruction chain and then truth information is used to select muons from numuCC interactions which are eligible for MCS analysis. The SAM definition used for this sample is "prodgenie_bnb_nu_uboone_mcc7_reco2".

4.2 Fiducial Volume Definition

The MicroBooNE TPC has active volume dimensions of 2.6 m width $\times$ 2.3 m height $\times$ 10.4 m length. For this analysis, a smaller "fiducial volume" is defined and referenced throughout this note (for example, in many cases reconstructed tracks are required to be fully contained within the fiducial volume). For reference, the fiducial volume definition used throughout this note is the full TPC volume reduced in by 20 cm from both the cathode plane and the anode wire planes, shifted in 26.5 cm in from both the top and bottom walls of the TPC, shifted in 20 cm from the beam-upstream wall of the TPC, and shifted in 36.8 cm from the downstream wall of the TPC. The reason for this choice of fiducial volume is that it reduces contamination from "edge effects" that occur near the walls of the TPC, like electric field distortions and space-charge effects. While the TPC has a total active volume of 62.6 m^3, the fiducial volume used in this analysis has a volume of 38.7 m^3 or roughly 62% of the total TPC active volume.

4.3 Performance with MCTracks

4.3.1 MCTrack Description

MCTrack objects are made from the output of geant4, and are created from geant4 energy depositions in the detector. geant4 outputs 3D energy depositions in the detector, along with truth information about which parent particles deposited this energy. MCTracks are 3D objects which are formed by grouping the energy depositions based on parent particles. Whether a particle in geant4 is turned into an MCTrack or an MCShower (not discussed in this note) is based on truth PDG (for example, muons, protons, and pions always form MCTracks).

Each MCTrack is itself a vector of 3D trajectory points, which are ordered to match the direction of the particle that deposited the energy. Trajectory points are only formed for energy depositions inside of the TPC volume. In general, long MCTracks will have steps separated by up to several centimeters. Each step in an MCTrack holds the following information used in this analysis: 3D position, and true energy at that point. Only information within the realm of reconstructable quantities is used in this analysis, with the exception of true energy (which is used for example to quantify a reconstructed energy resolution).

Since the output of a nominal reconstruction chain (including hit finding, clustering, matching across planes, etc.) are 3D tracks, MCTracks can be studied in an analysis in the exact same way as a reconstructed track would be. MCTracks can be thought of as perfectly reconstructed tracks, where each trajectory point along the track is a true 3D energy deposition inside of the MicroBooNE TPC.

Since MCTracks are formed from true 3D energy depositions and not from wire signals on drift electrons, MCTracks are insensitive to broken wires, noise, and other simulated detector effects.

It is worth noting that delta rays eminating from muon tracks are relevant for MCS calculations. Here, delta rays form MCShowers and are therefore invisible to this analysis. This is the same as assuming the reconstructed tracks have perfectly removed charge from delta rays in their algorithms.

4.3.2 Event Selection

The event selection for this subanalysis is truth based. The fiducial volume used in this subanalysis is the same as is used throughout the note, defined in Section 4.2. Beginning with the 772,000 events in the sample, the cuts placed are:

- There is one neutrino interaction in the event (770,241 events remain).
- The neutrino interaction is of type charged-current (559,348 events remain).
- The neutrino interaction occurs within the fiducial volume (152,214 events remain) (note the large decrease in statistics because these neutrinos were generated within the full cryostat, and the fiducial volume is much smaller).
- The interacting neutrino is type ν_μ (149,684 events remain).
- The MCTrack associated with the outgoing muon from the interaction is fully contained within the fiducial volume (50,537 events remain).
- The MCTrack associated with the outgoing muon from the interaction is at least one meter in length (23,378 events remain).
- The MCTrack associated with the outgoing muon from the interaction does not decay in flight (this cut is implemented by requiring the MCTrack's total energy at its final trajectory point is equal to the muon mass) (23,342 events remain).

After these additional cuts are placed, 23342 events (MCTracks) remain for MCS analysis. The energy and angle distributions for these 23342 muons can be seen in Figure 3. It should be noted that any computed metrics from this sample (and therefore any other BNB sample) have convolved any effects of performance differences as a function of angle. While MCTracks do not generally suffer from problems related to angle, reconstructed tracks do (since reconstructing 3D tracks that have certain angles with

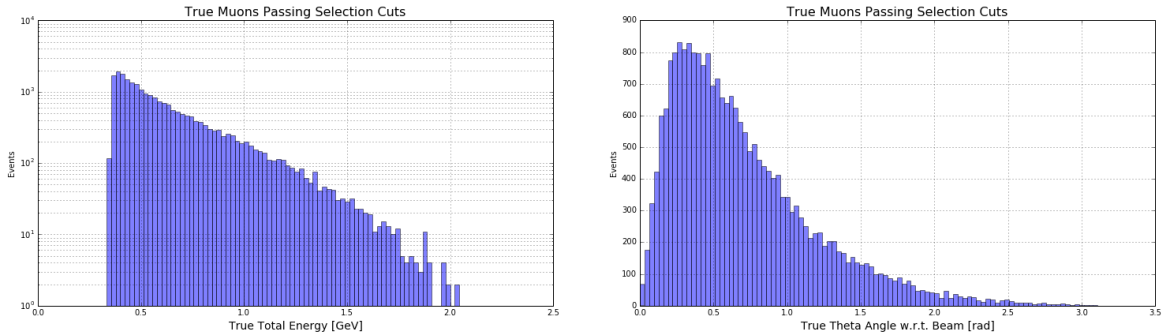

(a) *Muon energy distribution.*

(b) *Muon theta angle (angle with respect to the beam direction) distribution.*

Figure 3: *Energy and angle distributions for muons from numuCC interactions in MicroBooNE simulation passing cuts described in Section 4.3.2.*

respect to wire planes can be difficult). The effect that reconstructed track angle has on MCS performance is explored briefly in Appendix E.

4.3.3 Range Energy Validation

With this sample of MCTracks, it is possible to quantify MCS energy (momentum) resolution as a function of true energy (momentum). However, in actual MicroBooNE data there is obviously no true momentum with which to compare. The additional momentum handle that is used in data for contained tracks is range-based energy. The stopping power of muons in liquid argon is well described by the particle data group[13]. By using a linear interpolation between points in the cited PDG stopping power table, the start-to-end straight-line length of a track can be used to reconstruct the muon's total energy with good accuracy. Figure 4 shows a comparison of range energy to true energy for this sample.

In order to compute a bias and a resolution, Figure 4 is sliced in bins of true muon energy and a histogram of the fractional energy difference ($\frac{E_{range}-E_{true}}{E_{true}}$) is created for each bin. This distribution is shown for three representative bins in Figure 5, along with the gaussian fit to each. The mean (μ) of each gaussian fit is used to compute a bias as a function of true energy, while the width (σ) of each distribution is used to compute a resolution. Figure 6 shows the bias and resolution for the range-based energy reconstruction method. It can be seen that the bias is negligible and the resolution for this method of energy reconstruction is on the order of 2-4%. Based on this figure, it is clear that range-based energy (and therefore range-based momentum) is a good handle on the true energy (momentum) of a reconstructed muon track in MicroBooNE data, assuming that track is well reconstructed in terms of length.

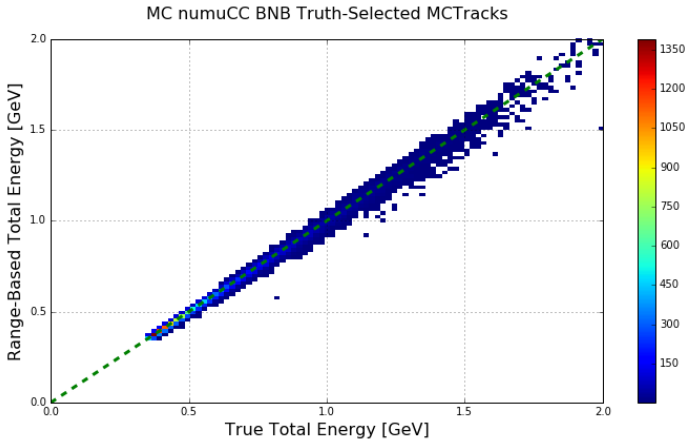

Figure 4: *Range based energy versus true energy for the* MCTrack *sample described in Section 4.3.2.*

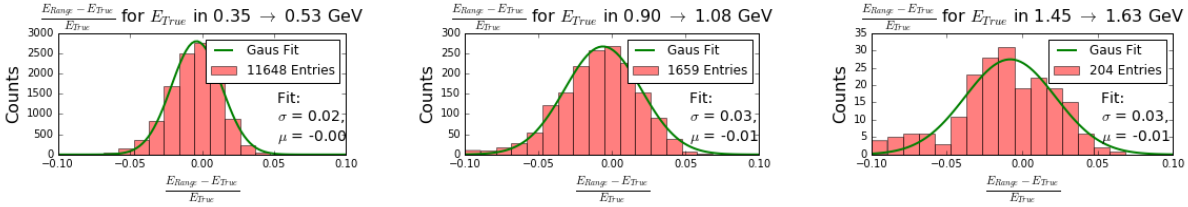

(a) *Fractional energy difference between 0.35 and 0.53 GeV true energy.*

(b) *Fractional energy difference between 0.90 and 1.08 GeV true energy.*

(c) *Fractional energy difference between 1.45 and 1.63 GeV true energy.*

Figure 5: *Fractional energy difference for a few representative bins of true energy derived from Figure 4.*

4.3.4 MCS Momentum Validation

For this sample of MCTracks, only the 3D trajectory points of each MCTrack are used as input to the MCS code, described in Section 3. The resulting MCS momentum versus range-based momentum can be seen in Figure 7. Range momentum is used here instead of true momentum in order to make this plot more directly comparable with the same analysis on data where true momentum is not accessible. In order to compute a bias and a resolution, Figure 7 is sliced in bins of range momentum and a histogram of the fractional momentum difference ($\frac{p_{MCS}^{-1} - p_{range}^{-1}}{p_{range}^{-1}}$) is created for each bin[6]. This distribution is shown for three representative bins in Figure 8, along with the gaussian fit to each. The mean (μ) of each gaussian fit is used to compute a bias as a function of range momentum, while the width (σ) of each distribution is used to compute a resolution. The bias and resolution for this momentum reconstruction method shown in Figure 9. This figure indicates a bias in the MCS momentum resolution on the order of a few percent, with a resolution that decreases from about 9% for contained MCTracks with true

[6]The choice of using inverse momentum is justified in Appendix D.

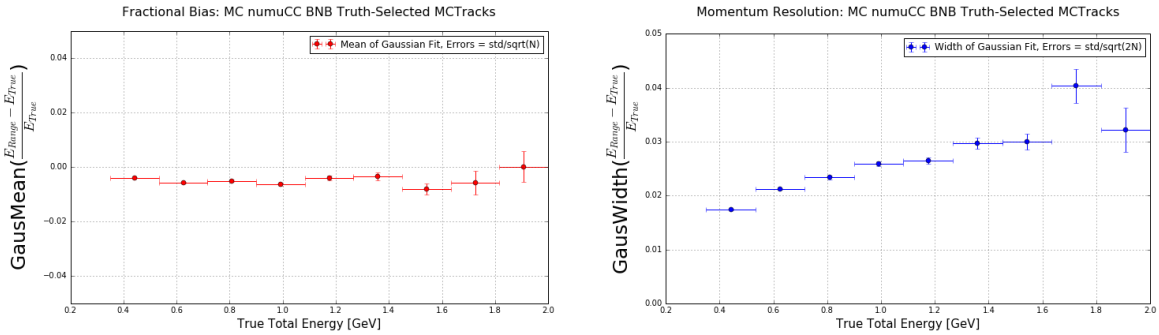

(a) *Range energy bias as a function of true energy. The vertical error bars are computed as* $\frac{\sigma_{fit}}{\sqrt{N}}$*, and the horizontal error bars indicate bin width.*

(b) *Range energy resolution as a function of true energy. The vertical error bars are computed as* $\frac{\sigma_{fit}}{\sqrt{2N}}$*, and the horizontal error bars indicate bin width.*

Figure 6: *Range energy and true energy bias and resolution for the* MCTrack *sample described in Section 4.3.2.*

391 total momentum around 0.5 GeV (which corresponds to a length of about 1.7 meters) to below 3% for
392 contained MCTracks with true total momentum greater than 0.8 GeV (which corresponds to a length
393 of about 3.1 meters).

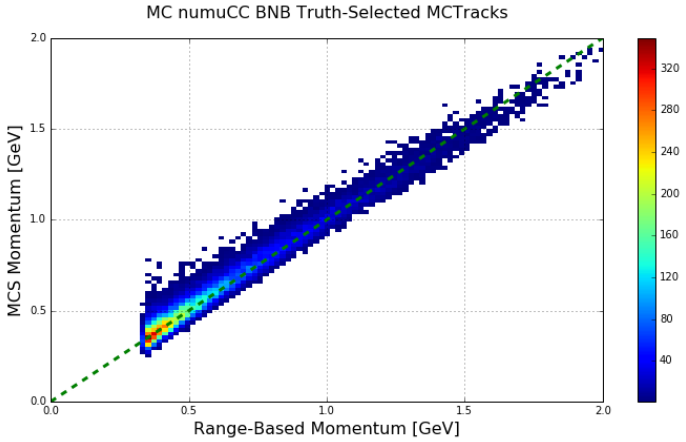

Figure 7: *MCS computed momentum versus range momentum for the* MCTrack *sample described in Section 4.3.2. Note the cutoff at around 0.3 GeV range-based momentum is caused by the minimum track length of 100 centimenter requirement.*

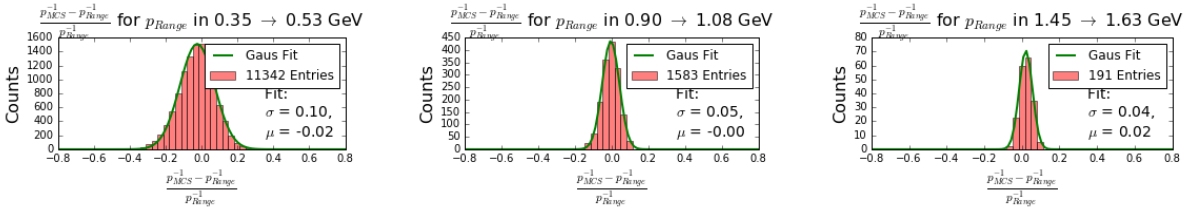

(a) *Fractional momentum difference between 0.35 and 0.53 GeV range momentum.*

(b) *Fractional momentum difference between 0.90 and 1.08 GeV true momentum.*

(c) *Fractional momentum difference between 1.45 and 1.63 GeV true momentum.*

Figure 8: *Fractional momentum difference for a few representative bins of range momentum derived from Figure 7.*

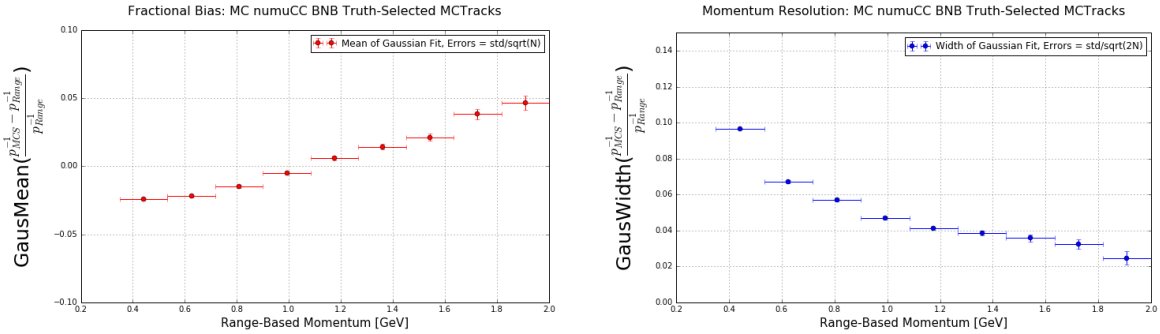

(a) *MCS momentum bias as a function of range momentum. The vertical error bars are computed as* $\frac{\sigma_{fit}}{\sqrt{N}}$*, and the horizontal error bars indicate bin width.*

(b) *MCS momentum resolution as a function of range momentum. The vertical error bars are computed as* $\frac{\sigma_{fit}}{\sqrt{2N}}$*, and the horizontal error bars indicate bin width.*

Figure 9: *MCS momentum bias and resolution as a function of range momentum for the* MCTrack *sample described in Section 4.3.2.*

4.3.5 Highland Validation

For a given track segment momentum and length, 98% of the angular scatter deviations should be gaussian with an RMS described by the Highland equation (Equation 2), while the remaining 2% are larger angle Rutherford scatters[3][7]. Therefore, a histogram of track segment angular deviations divided by the RMS predicted by the Highland equation should be gaussian with a width of unity. In this section, we validate this claim.

For each 10 cm segment of each MCTrack in this single muon sample, the momentum of the muon at the start of that segment is estimated by taking the computed MCS momentum and subtracting out momentum lost in the track upstream of the start of this segment, assuming the track was minimally ionizing as described in Equation 8. The segment momentum, along with the segment length, is converted into an expected RMS angular deviation by way of Equation 2. For each consecutive pair of segments, the angular scatter in milliradians divided by the Highland expected RMS in millradians is an entry in the histogram shown in Figure 10. From this figure we can see that the Highland formula is valid for MCTracks, as the gaussian fit agrees well with the underlying histogram. One can also see the non-gaussian tails which may correspond to larger angle Rutherford scatters.

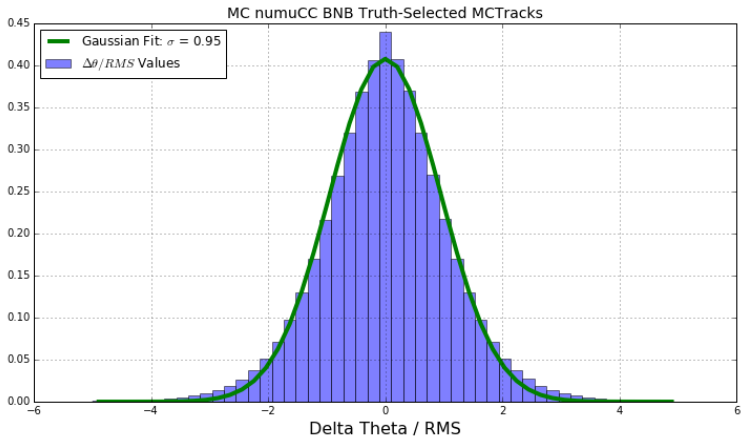

Figure 10: *10 cm segment angular deviations divided by expected Highland RMS for the single muon* MCTrack *sample described in Section 4.3.2.*

4.4 Performance with Reconstructed Tracks

4.4.1 Event Selection

The event selection for this subanalysis is identical to that described in Section 4.3.2 with one additional cut. The additional cut is requiring that there is a reconstructed track which starts within 3 cm of the start and ends within 3 cm of the end of the aforementioned MCTrack (or vice-versa). This cut is

[7] This is not actually taken into account explicitly in the current algorithm implementation

requiring that the track is well reconstructed in terms of position (direction is taken into account later). 13810 events pass this cut, down from the 23342 previously.

4.4.2 MCS Momentum Validation

For this sample of reconstructed tracks, only the 3D trajectory points of each reconstructed track are used as input to the MCS code, described in Section 3. The resulting MCS momentum versus range-based momentum for this sample of reconstructed tracks without any cuts other than those described in Section 4.4.1 can be seen in Figure 11.

In order to compute a bias and a resolution, Figure 11 is sliced in bins of range momentum and a histogram of the fractional momentum difference ($\frac{p_{MCS}^{-1} - p_{range}^{-1}}{p_{range}^{-1}}$) is created for each bin[8]. This distribution is shown for three representative bins in Figure 12, along with the gaussian fit to each. The mean (μ) of each gaussian fit is used to compute a bias as a function of range momentum, while the width (σ) of each distribution is used to compute a resolution. The bias and resolution for this momentum reconstruction method shown in Figure 13. This figure indicates a bias in the MCS momentum resolution on the order of a few percent, with a resolution that decreases from about 9% for contained tracks with true total momentum around 0.5 GeV (which corresponds to a length of about 1.7 meters) to below 7% for contained tracks with true total momentum greater than 0.8 GeV (which corresponds to a length of about 3.1 meters). This agrees reasonably well with the analogous plots created from simulated single muons with MCTracks (Figure 9).

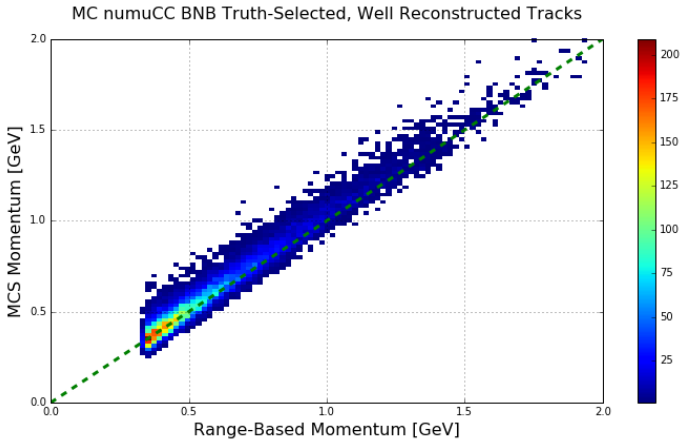

Figure 11: *MCS computed momentum versus range momentum for the truth-selected simulated fully contained, well reconstructed muon tracks from numu charged current events.*

[8]The choice of using inverse momentum is justified in Appendix D

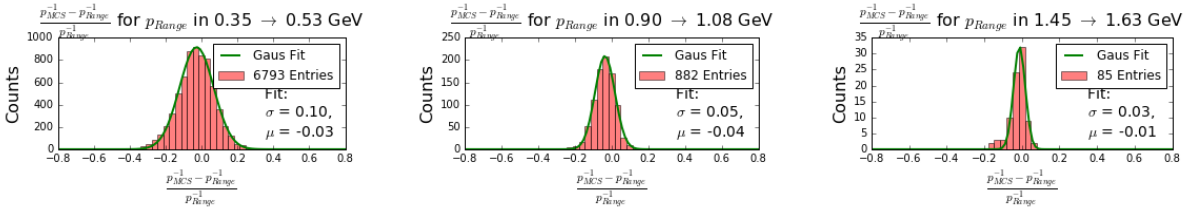

(a) *Fractional momentum difference between 0.35 and 0.53 GeV range momentum.*

(b) *Fractional momentum difference between 0.90 and 1.08 GeV range momentum.*

(c) *Fractional momentum difference between 1.45 and 1.63 GeV range momentum.*

Figure 12: *Fractional momentum difference for a few representative bins of range momentum derived from Figure 11.*

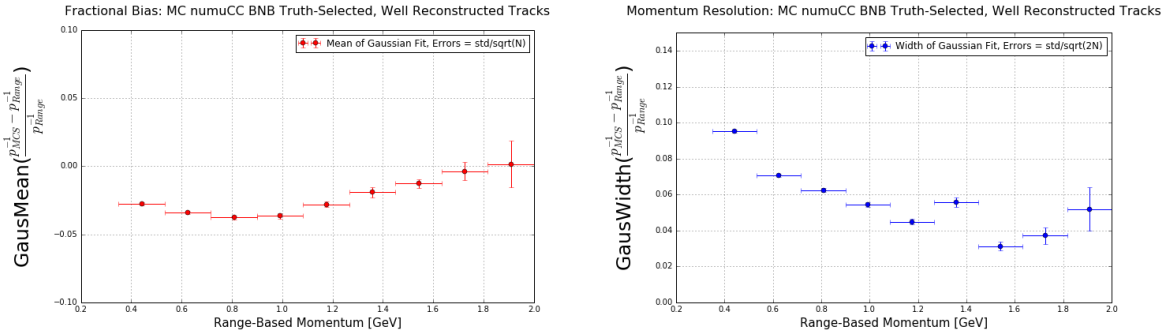

(a) *MCS momentum bias as a function of range momentum. The vertical error bars are computed as* $\frac{\sigma_{fit}}{\sqrt{N}}$*, and the horizontal error bars indicate bin width.*

(b) *MCS momentum resolution as a function of range momentum. The vertical error bars are computed as* $\frac{\sigma_{fit}}{\sqrt{2N}}$*, and the horizontal error bars indicate bin width.*

Figure 13: *MCS momentum bias and resolution as a function of range momentum for the truth-selected simulated fully contained, well reconstructed muon tracks from numu charged current events.*

4.4.3 Highland Validation

For this sample of tracks, the same Highland validation plot is created in exactly the same way as described in Section 4.3.5. For each consecutive pair of segments, the angular scatter in milliradians divided by the Highland expected RMS in millradians is an entry in the histogram shown in Figure 14. From this figure we can see that the Highland formula is valid for well reconstructed tracks in simulation when 10 cm segments are used.

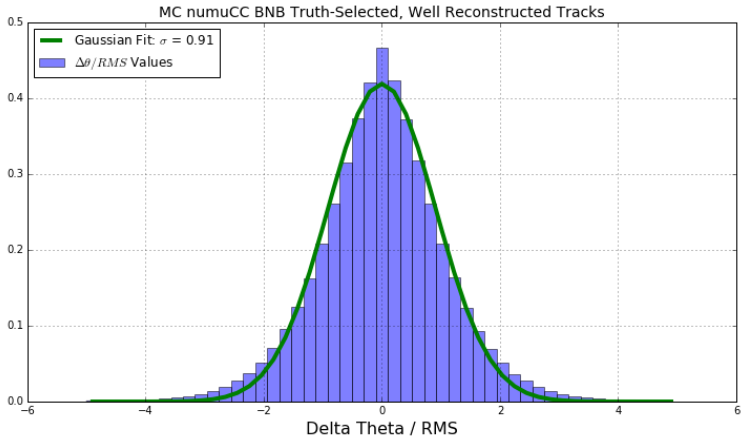

Figure 14: *10 cm segment angular deviations divided by expected Highland RMS for the sample of well reconstructed, neutrino induced muons in simulation.*

5 MCS Performance on Automatically Selected Muons from numuCC Events With Cosmics in Simulation

5.1 Input Sample

The input sample to this portion of the analysis is roughly 190,000 MCC7 simulated BNB neutrino interactions with CORSIKA cosmics as used by the CCInclusive group and descibed in their interal note[14]. These simulated events are run through a fully automated reconstruction chain and then a fully automated event selection routine described in Section 5.2. The SAM definition used for this sample is "prodgenie_bnb_nu_cosmic_uboone_mcc7_reco2".

5.2 Event Selection

The event selection algorithms used are designed to locate ν_μ charged-current interactions, where at least one muon track exits the interaction vertex. The event selection is described in detail in Section 6.2.1 of the MicroBooNE CCInclusive internal note ("Selection IIA: track multiplicity 2 (or larger) and no containment requirement")[14] but the main points will be recapped here. The selection takes as input reconstructed vertices created by the "pmtrack" producer module, reconstructed tracks created by the "pandoraNuPMA" track producer module, and optical hits produced by the "opFlashSat" producer module. The fiducial volume used in this subanalysis is the same as is used throughout the note, defined in Section 4.2. The following selection cuts are placed to isolate ν_μ charged-current interactions, and their efficiencies are documented in the aforementioned CCInclusive internal note:

1. The event must have at least one flash inside of the BNB beam-spill window brighter than 50 PE.
2. Two or more reconstructed tracks must originate from the same reconstructed vertex within the fiducial volume (defined in Section 4.2).
3. The tracks must overlap within a 70 cm buffer in the drift (z) direction of the center of the reconstructed optical flash.
4. For events with exactly two tracks originating from the vertex, additional calorimetric-based cuts are applied to mitigate backgrounds from in-time cosmics which produce Michel electrons that get reconstructed as a track.

After these event selection cuts are placed, the sample size is 15286 events. Further cuts are placed to isolate single tracks that are eligible for this MCS analysis.

1. The longest track is assumed to be the muon, and it is the only track studied in this analysis.
2. This track must be fully contained within the fiducial volume (6384 events remain).
3. This track must be at least one meter in length (2406 events remain).
4. This track must match with an MCTrack (Section 4.3.1) originating from the true neutrino interaction in the event. Here, "match" means that the start of the reconstructed track is within 3 cm of the start of the MCTrack, and the end of the reconstructed track is within 3 cm of the end of the MCTrack (or vice-versa). Note this removes any cosmic-induced mis-identifications. (1613 events remain).

After these additional cuts are placed, 1613 events (tracks) remain for MCS analysis. It should be known that there are some inherent pion and proton mis-identification (MID) backgrounds in this sample

after these cuts are placed. 88% of the time the identified track is truly a muon. Protons and pions make up the remaining MIDs with 8.6% and 3.4% respectively.

5.3 MCS Momentum Validation

The MCS momentum versus range-based momentum without any cuts other than those described in Section 5.2 can be seen in Figure 15. The off-diagonal component visible in this figure (where MCS momentum overestimates range momentum) is caused primarily by MIDs, most commonly where the longest track is a proton. Those familiar with this analysis may see the off diagonal component and associate it with "broken tracks" (tracks which are reconstructed as starting in the correct place but stopping prematurely, thus having a range-based momentum which disagrees with the true momentum), but note that there are no "broken tracks" in this figure because of the track-MCTrack matching requirement described in Section 5.2. Figure 16 divides Figure 15 into those events in which the MCTrack matched to the reconstructed track is a proton, a pion, or a muon. From this figure it is clear comparing MCS momentum to range momentum for contained tracks will provide a handle on separating muon tracks from proton tracks in data (though it is hard to make similar conclusions about pions due to limited statistics in this study).

The bias and resolution for the MCS momentum estimation method on this sample is computed in the same way as described in previous sections (for example in Section 4.4.2). Note that only those events in which the reconstructed track corresponds to a muon in truth (Figure 16(c)) are used to compute bias and resolutions. The bias and resolution for this momentum reconstruction method is shown in Figure 18. This figure indicates a bias in the MCS momentum resolution on the order of a few percent, with a resolution that decreases from about 10% for contained tracks with true total momentum around 0.5 GeV (which corresponds to a length of about 1.7 meters) to below 7% for contained tracks with true total momentum greater than 0.8 GeV (which corresponds to a length of about 3.1 meters). This agrees well with the analogous plots created from simulated single muons with reconstructed tracks (Figure 13).

5.4 Highland Validation

For this sample of contained, automatically selected, well-reconstructed neutrino-induced tracks, the same Highland validation plot is created in exactly the same way as described in Section 4.3.5. For each consecutive pair of segments, the angular scatter in milliradians divided by the Highland expected RMS in millradians is an entry in the histogram shown in Figure 19. From this figure we can see that the Highland formula is valid for automatically selected, well reconstructed neutrino-induced muon tracks in simulation.

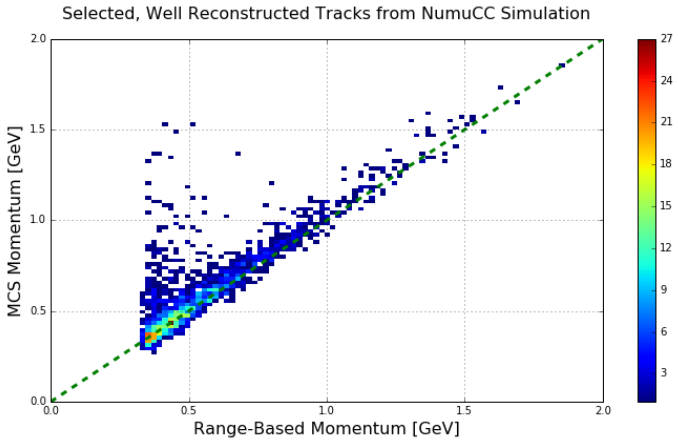

Figure 15: *MCS computed momentum versus range momentum for the automatically selected simulated neutrino-induced fully contained, well reconstructed muon sample without any additional cuts to mitigate MIDs.*

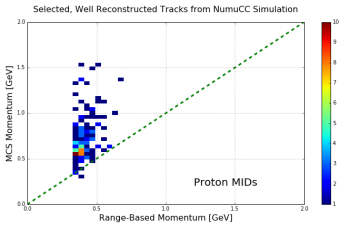

(a) *The subset of events in Figure 15 in which the true identity of the track is a proton.*

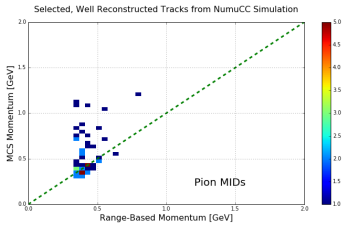

(b) *The subset of events in Figure 15 in which the true identity of the track is a pion.*

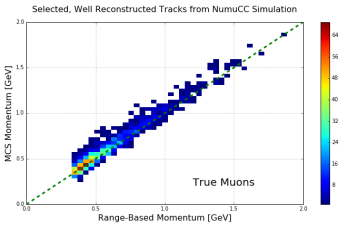

(c) *The subset of events in Figure 15 in which the true identity of the track is a muon.*

Figure 16: *MCS computed momentum versus range momentum for the selected neutrino-induced, well reconstructed fully contained muon sample in simulation broken up by true particle identity of the track.*

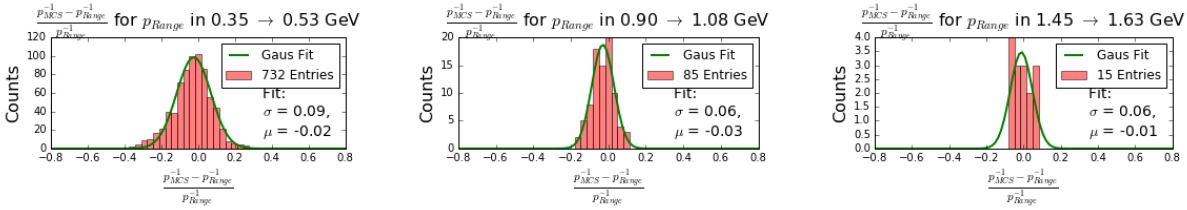

(a) *Fractional momentum difference between 0.35 and 0.53 GeV range momentum.*

(b) *Fractional momentum difference between 0.90 and 1.08 GeV range momentum.*

(c) *Fractional momentum difference between 1.45 and 1.63 GeV range momentum.*

Figure 17: *Fractional momentum difference for a few representative bins of range momentum derived from Figure 16(c) (which is produced using only those tracks which truly match to a muon).*

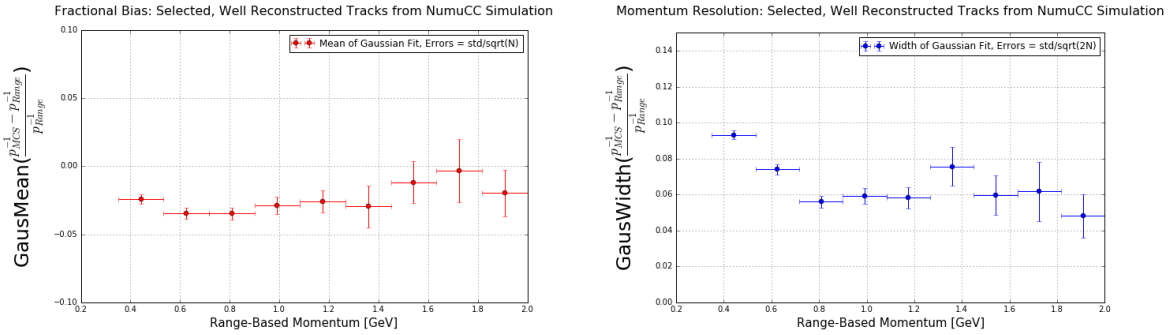

(a) *MCS momentum bias as a function of range momentum. The vertical error bars are computed as* $\frac{\sigma_{fit}}{\sqrt{N}}$*, and the horizontal error bars indicate bin width.*

(b) *MCS momentum resolution as a function of range momentum. The vertical error bars are computed as* $\frac{\sigma_{fit}}{\sqrt{2N}}$*, and the horizontal error bars indicate bin width.*

Figure 18: *MCS momentum bias and resolution as a function of range momentum for the selected, well reconstructed neutrino-induced muons in MicroBooNE simulation.*

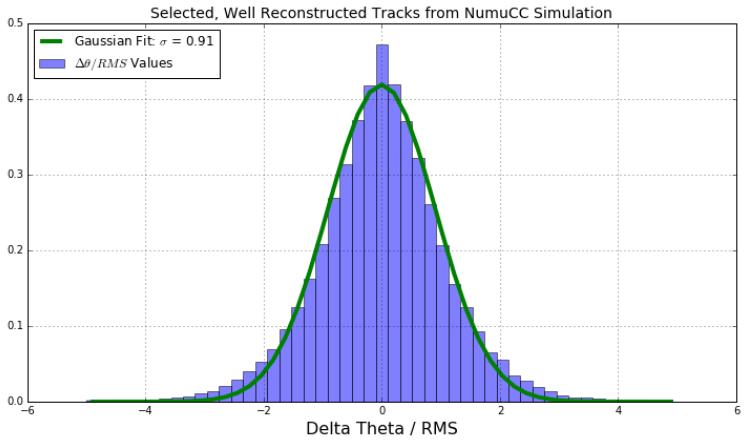

Figure 19: *10 cm segment angular deviations divided by expected Highland RMS for the sample of well reconstructed, neutrino induced muons in simulation.*

6 MCS Performance on Automatically Selected Muons from numuCC Events in MicroBooNE Data

6.1 Input Sample

The input sample to this portion of the analysis is roughly 5e19 POT worth of triggered BNB neutrino interactions in MicroBooNE data as used by the CCInclusive group and descibed in their interal note[14]. These events are run through the same fully automated reconstruction chain and event selection routine described in Section 5.1. The SAM definition used for this sample is "prod_bnb_reco_neutrino2016_beamfilter_goodruns_v5".

6.2 Event Selection

The exact same event selection cuts are used to identify ν_μ charged-current events in this data sample as described in Section 5.2. The fiducial volume used in this subanalysis is the same as is used throughout the note, defined in Section 4.2. The same further cuts to isolate the subset of those events viable for MCS analysis are also placed, with the exception of the cut requiring the reconstructed track matches well with an MCTrack in the event (as there are no MCTracks in real data). In order to accommodate for this difference, a hand scan of the selected events was conducted.

After the event selection cuts, the minimum track length cut, and the containment cuts were placed, 598 events (tracks) remained. Each of these events (tracks) were scanned by hand with an interactive event display. What was shown to the scanner (David Kaleko) were three two-dimensional displays with the raw-wire signals on them. Overlaid on each display was the 2D projection of the 3D reconstructed track and vertex. The scanner looked to ensure the track was well reconstructed (it started within a few cm of the vertex and ended within a few cm of the end of the wire-signal track or vice-versa in all three planes). Additionally the scanner looked for obvious MID topologies like cosmic rays inducing Michel electrons at the reconstructed neutrino vertex (for example when a clear Bragg peak is visible at the neutrino vertex) and also for obvious MID topologies where the track is likely a pion (for example if it charge-exchanges and creates a clear neutral pion decay topology). In general, the scanner chose to be conservative in the sense that if the track didn't look very clearly like a muon from a ν_μ charged-current event, the track (event) was removed from the analysis. The purpose of searching for MIDs is to attempt to reproduce the truth-based removal of cosmic, pion, and proton MIDs that is ultimately done in Section 5 so as to make an apples-to-apples data/MC comparison.

A sample event that was removed by the hand scanner is shown in Figure 20. Only one two-dimensional display is shown (from the collection plane wires), while the 2D projection of the 3D track is shown in black. The 2D projection of the 3D reconstructed neutrino vertex is shown as a small cyan dot near the bottom left of the image. It is clear that the reconstructed track starts in the correct place, but it is truncated and stops before the end of the track. This track was deemed "poorly reconstructed" and was therefore removed from the analysis. A second sample event that was removed by the hand scanner is shown in Figure 21. This event was deemed some form of unknown MID. The reconstructed track matches wire signals well, but this event does not appear to be a clean ν_μ charged-current event, with at least one neutral pion decay visible near the center of the track. A sample event that was deemed acceptable is shown in Figure 22.

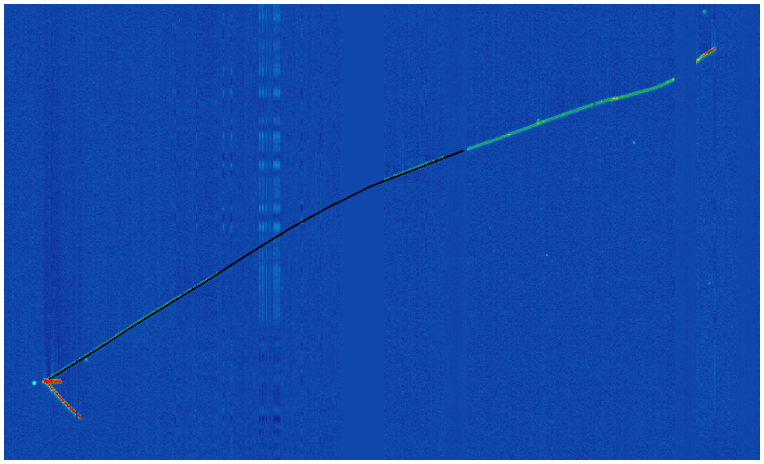

Figure 20: *A hand-scanned data event that was deemed "poorly reconstructed" and removed from this analysis. The 2D projection of the 3D reconstructed track (shown in black overlaid on raw wire signals) clearly stops before it reaches the end of the particle's trajectory.*

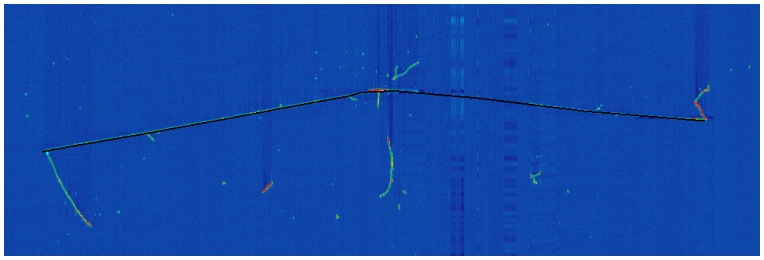

Figure 21: *A hand-scanned data event that was deemed some form of MID and removed from this analysis. The 2D projection of the 3D reconstructed track (shown in black overlaid on raw wire signals) matches raw wire signals well, but this event does not appear to be a clean ν_μ charged-current event, with at least one neutral pion decay visible near the center of the track.*

6.3 MCS Momentum Validation

The MCS momentum versus range-based momentum *without any additional hand-scan reconstruction quality checks* can be seen in Figure 23. The off-diagonal component visible in this figure (where MCS momentum greatly overestimates range momentum) is caused both by poor track reconstruction (truncated tracks) and MIDs. Figure 24 divides Figure 23 into those events which are handscanned as having poorly reconstructed or obviously MID'd tracks, and those which are well reconstructed. It can be seen that hand-scanning tends to remove the off-diagonal component and therefore improve the MCS momentum resolution. Note that only those events which have been hand-scanned as acceptable (Figure 24(b)) will be used to compute bias and resolutions.

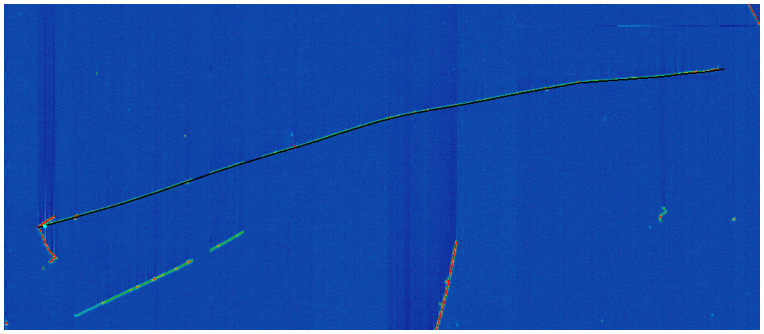

Figure 22: *A hand-scanned data event that was deemed acceptable for MCS analysis. The track looks well reconstructed, and the wire signals indicate that the particle is likely a muon, and a clear Bragg peak can be seen at the end of the track indicating the track is well contained.*

559

560 The bias and resolution for this momentum reconstruction method shown in Figure 26. This figure
561 indicates a bias in the MCS momentum resolution on the order of a few percent, with a resolution that
562 decreases from about 11% for contained reconstructed tracks with range momentum around 0.5 GeV
563 (which corresponds to a length of about 1.7 meters) to about 7% for contained reconstructed tracks
564 with range momentum greater than 0.8 GeV (which corresponds to a length of about 3.1 meters). This
565 is only slightly higher than the the same bias and resolution measurement in simulation as shown in
566 Figure 18, a difference which may be attributed to the inefficiencies in hand scanning (as compared to
567 the truth-based MID removal and track-well-reconstructed checks in simulation-based sections). Note
568 the bias and resolution plots here stop at a maximum range-based momentum of below 1.4 GeV due to
569 limited statistics.

570 ## 6.4 Highland Validation

571 For this sample of contained, selected, well-reconstructed neutrino-induced tracks in MicroBooNE data,
572 the same Highland validation plot is created in exactly the same way as described in Section 4.3.5. For
573 each consecutive pair of segments, the angular scatter in milliradians divided by the Highland expected
574 RMS in millradians is an entry in the histogram shown in Figure 27, both for the tracks hand scanned as
575 being well reconstructed, and for the sample rejected by the hand scanner as being poorly reconstructed
576 or having obvious MID topologies. From this figure we can see that the Highland formula is valid for
577 well reconstructed, contained muon tracks in data.

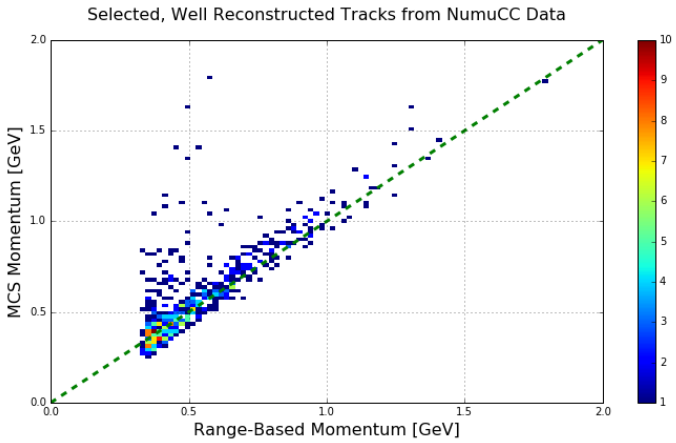

Figure 23: *MCS computed momentum versus range momentum for the selected neutrino-induced fully contained muon sample in data without any additional handscanning to check for reconstruction quality. The off-diagonal where MCS momentum greatly overestimates range momentum is caused by poor track reconstruction (truncated tracks) and MIDs.*

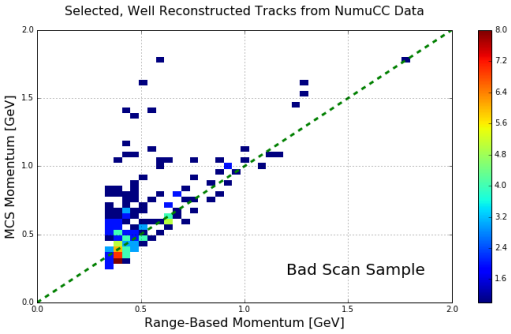

(a) *The subset of events in Figure 23 which were handscanned as having poor reconstruction quality or having obvious MID topologies.*

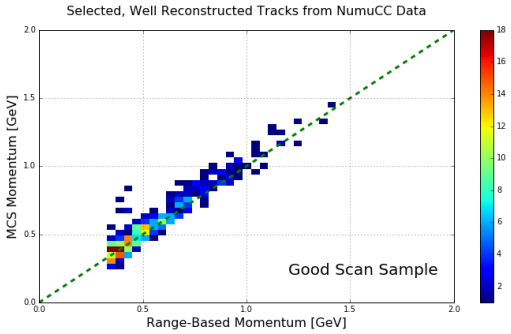

(b) *The subset of events in Figure 23 which were handscanned as having good reconstruction quality or having obvious MID topologies.*

Figure 24: *MCS computed momentum versus range momentum for the selected neutrino-induced fully contained muon sample in data hand-scanned as having poorly reconstructed tracks (left) and well reconstructed tracks (right).*

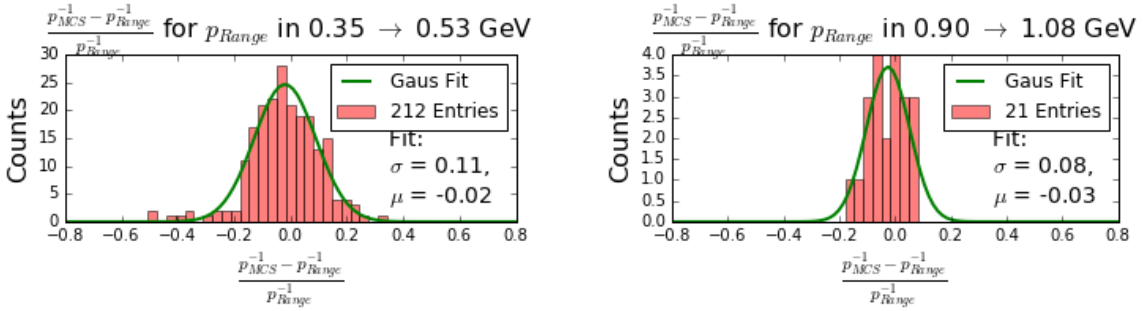

(a) *Fractional momentum difference between 0.35 and 0.53 GeV range momentum.*

(b) *Fractional momentum difference between 0.90 and 1.08 GeV range momentum.*

Figure 25: *Fractional momentum difference for a few representative bins of range momentum derived from Figure 24(b).*

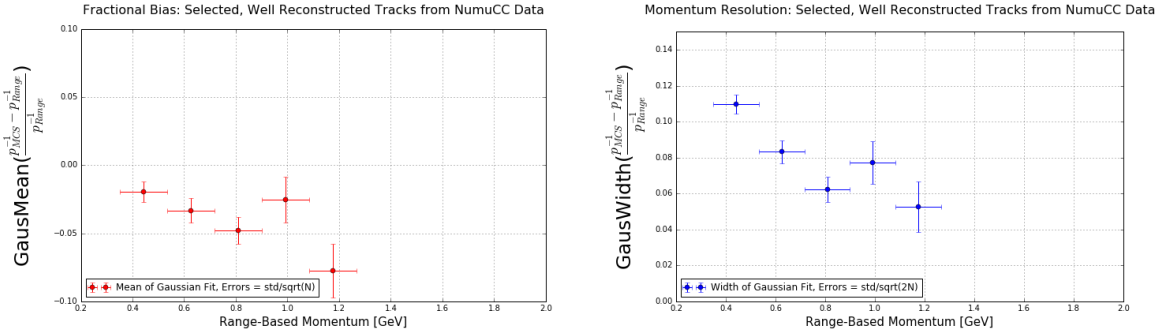

(a) *MCS momentum bias as a function of range momentum. The vertical error bars are computed as* $\frac{\sigma_{fit}}{\sqrt{N}}$*, and the horizontal error bars indicate bin width.*

(b) *MCS momentum resolution as a function of range momentum. The vertical error bars are computed as* $\frac{\sigma_{fit}}{\sqrt{2N}}$*, and the horizontal error bars indicate bin width.*

Figure 26: *MCS momentum bias and resolution as a function of range momentum for the selected, well reconstructed neutrino-induced muons in MicroBooNE data.*

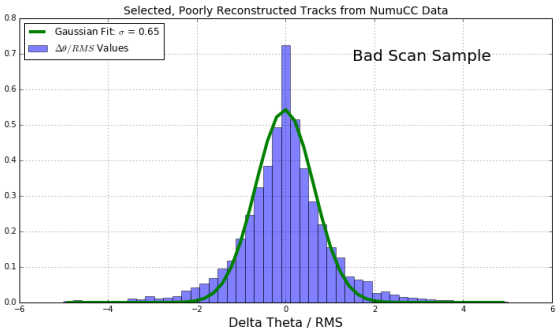

(a) *The MicroBooNE data sample handscanned as being poorly reconstructed.*

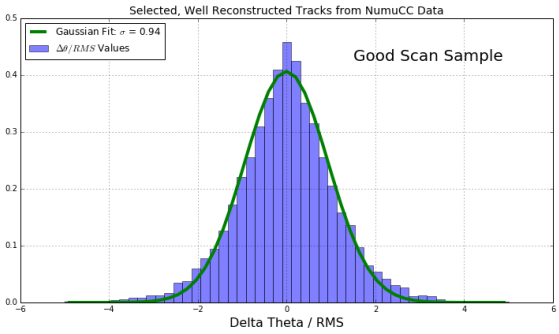

(b) *The MicroBooNE data sample handscanned as being well reconstructed or being a MID topology.*

Figure 27: *10 cm segment angular deviations divided by expected Highland RMS for the sample of well reconstructed, neutrino induced muons in MicroBooNE data as well as for the sample deemed poorly reconstructed or MID topologies by the hand scanning.*

7 Conclusions and Outlook

This note has discussed the multiple coulomb scattering technique for estimating the momentum of a three dimensional reconstructed track and has provided motivation for demonstration of the capabilities of this tool within the neutrino LArTPC community. This technique will be important for future cross section and oscillation measurements from the MicroBooNE collaboration. The details of the implementation of this code have been described. The gaussian nature of scatters predicted by the Highland formula has been demonstrated. Additionally the performance of this method has been quantified in two different forms of simulation of fully contained tracks (truth-selected simulated BNB neutrino events with MCTracks and reconstructed tracks, and automatically-selected selected BNB + cosmic neutrino events) as well as in approximately 0.5e20 POT of MicroBooNE data.

To summarize the performance on the different fully contained track samples, the bias and resolution for the different samples are overlaid in Figure 28. In general, performance on reconstructed tracks in MC and data agree though extremely limited statistics above 1 GeV range-based momentum makes more concrete statements difficult. The energy resolution with reconstructed tracks tends to be slightly worse than that with MCTracks which can be attributed to imperfect track reconstruction and other detector effects to which MCTracks are insensitive like broken wires and simulated noise.

Other uses besides momentum reconstruction for the MCS technique have been described, including using it as a tool for identification of poorly reconstructed tracks and particle identification. In the appendices can be found descriptions of the methods used to optimize the segment length (10 cm) and detector resolution term (2 mrad) in the MCS algorithm, as well as studies of using MCS to determine track direction, and studies to justify using inverse momentum to compute bias and resolution metrics.

This note is by no means a complete, end-all analysis of the MCS code; there are many useful ways to continue this study. The most obvious example is the study of performance on exiting tracks. Only fully contained tracks have been studied here because the ultimate goal was to compare data to MC. Using only simulation, however, exiting tracks can be studied since truth energy is known. It is worth noting that Leonidas did a truncated-track analysis[9] in which he studied only the first n centimeters of a track to determine how the MCS resolution is impacted when the end of the track is not visible; in this way one is able to use fully contained tracks to mimic exiting ones and therefore still make data/MC comparisons. However, one has to keep in mind that the first one meter of a fully-contained 1 GeV muon does not behave the same as the first one meter of an exiting 2 GeV muon and therefore it is difficult to draw concrete conclusions about exiting tracks with this method. While contained tracks have a maximum energy determined by the size of the detector, exiting tracks are not limited in this way. A simulation-only study of exiting tracks is necessary and should be done.

Additional avenues to further this analysis include:

- Determining if the MCS algorithm can be used for muon/pion discrimination (pions should have more larger-angle hard scatters than muons).
- Quantifying the performance of the MCS algorithm as a function of track angle (which is briefly explored as an appendix to this note starting with version 1.4, but could be done more thoroughly).
- Using calorimetry to determine energy loss upstream of a segment rather than assuming average MIP deposited energy (Equation 8)... this will be best especially for cases where large amounts of

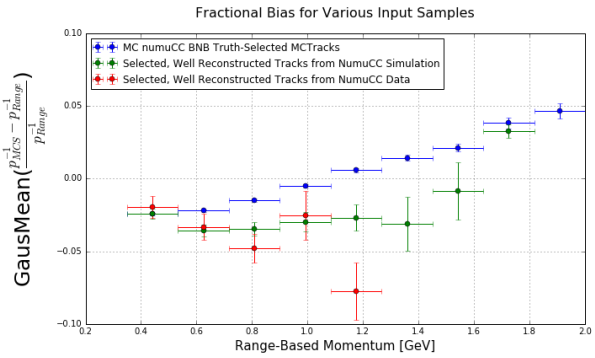

(a) *MCS momentum bias as a function of range momentum. The vertical error bars are computed as* $\frac{\sigma_{fit}}{\sqrt{N}}$*, and the horizontal error bars indicate bin width.*

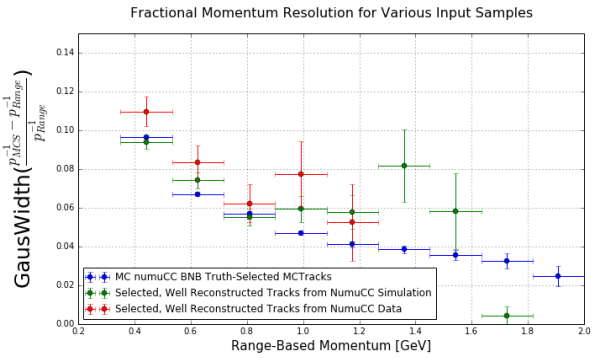

(b) *MCS momentum resolution as a function of range momentum. The vertical error bars are computed as* $\frac{\sigma_{fit}}{\sqrt{2N}}$*, and the horizontal error bars indicate bin width.*

Figure 28: *MCS momentum resolution for simulated truth-selected BNB numuCC* MCTracks *discussed in Section 4.3 (blue), automatically selected contained numuCC-induced muons from simulated BNB+cosmics where the track is well-reconstructed and matches with the true muon track discussed in Section 5 (green), and automatically selected contained numuCC-induced muons from MicroBooNE data where the track is deemed well-reconstructed and likely-muon from hand scanning discussed in Section 6.*

energy is lost to delta rays.

- Using a likelihood map (plot of likelihood vs. step in raster scan) to assign an uncertainty to the returned MCS momentum value (maybe something like the magnitude of the second derivative?)

8 Possible Plots for Publication

This section includes plots that to be considered for the publication. The publication should have its scope kept small so as to get it published in a very quick time scale. These plots of course can be modified, their captions changed, etc... I am just putting them here to paint a picture for the readers of this technote what I think should be included in the publication.

1. Figure 29 is a general image whose purpose is to aid the reader in understanding what MCS is and how the code works. I'm not sure this one is public-domain, but I can easily make my own version of it if necessary.
2. Figure 30 is an image whose purpose is to validate using range-based momentum in place of true-momentum when the analysis is done on real data where true-momentum obviously is unknown.
3. Figure 31 is an image whose purpose is to show that the segment-to-segment angular scatters are indeed gaussian as predicted by the Highland formula, and therefore the basis for this technique is sound.
4. Figure 32 is an image showing the MCS momentum versus range momentum for the automatically selected, handscanned data events.
5. Figure 33 is an overlay of MCS momentum bias and resolution for directly comparable samples in data and MC. The MCTrack sample is left out of this plot because MCTracks are very MicroBooNE specific. Also the x-axis cuts off at around 1.3 GeV as statistics become very limited after that.

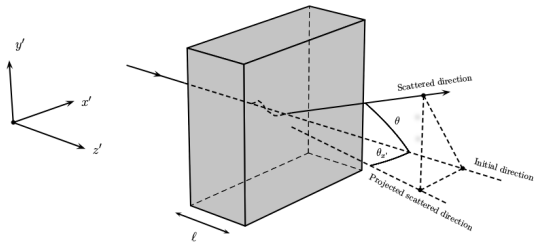

Figure 29: *The particle's trajectory is deflected as it traverses through the material [9].*

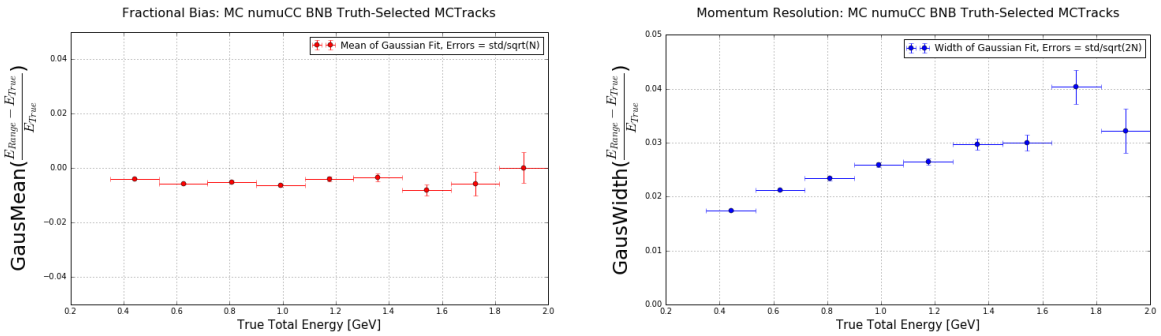

(a) *Range energy bias as a function of true energy.* (b) *Range energy resolution as a function of true energy.*

Figure 30: *Range energy and true energy bias and resolution for the* MCTrack *sample described in Section 4.3.2.*

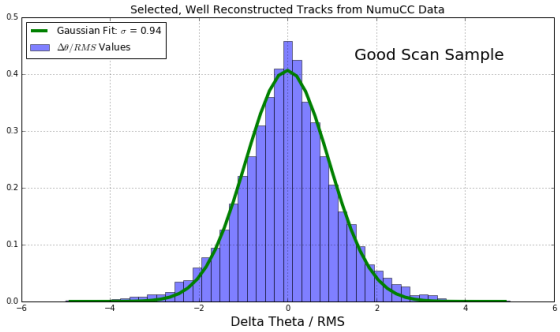

Figure 31: *10 cm segment angular deviations divided by expected Highland RMS for the sample of well reconstructed (as determined by the hand scanning), neutrino induced muons in MicroBooNE.*

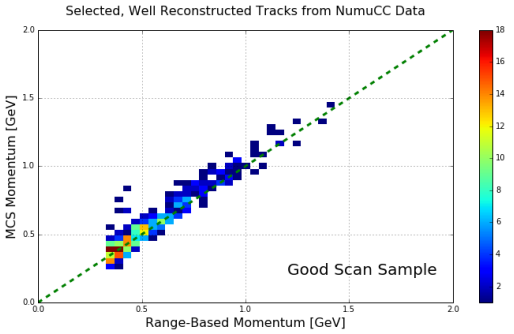

Figure 32: *MCS computed momentum versus range momentum for the selected neutrino-induced fully contained muon sample in data hand-scanned as having well reconstructed, likely-muon tracks.*

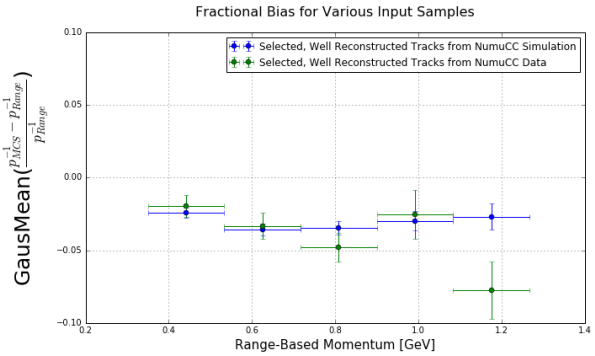

(a) *MCS energy bias as a function of range energy.*

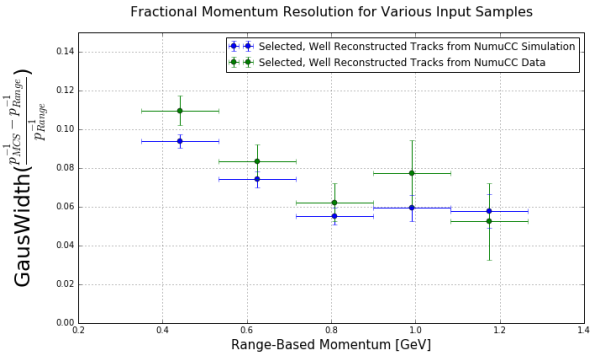

(b) *MCS energy resolution as a function of range energy.*

Figure 33: *MCS momentum resolution for automatically selected contained numuCC-induced muons from simulated BNB+cosmics where the track is well-reconstructed and matches with the true muon track discussed in Section 5 (blue), and automatically selected contained numuCC-induced muons from MicroBooNE data where the track is deemed well-reconstructed and likely-muon from hand scanning discussed in Section 6 (green).*

A Optimizing Segment Length

This section describes the study conducted to optimize the segment length in the algorithm. The input sample for this study was the high statistics simulated BNB neutrino interactions without any cosmics simulated described in Section 4.1, and this study uses reconstructed tracks that have been selected according to the cuts described in Section 4.4.1.

One of the tunable parameters in the MCS algorithm is the length of segments into which a track is divided. While shorter segment lengths yield more segments per track and therefore more sampling points to build a stronger likelihood, they also lead to the breakdown of the gaussian nature of scatters. Longer segments tend to have a more gaussian distribution of scatters but lead to fewer sampling points and therefore worse momentum resolution. Additionally, shorter segment lengths tend to have a higher momentum bias though why this is the case is not immediately obvious. For these reasons there exists an optimal segment length. Figure 34 shows analogous figures to Figure 14 for four different segment lengths ranging between 2 cm and 20 cm, with the same input sample of tracks. From this figure it can be seen that only segment lengths longer than or equal to 10 cm provide reasonably gaussian distributions. Figure 35 shows the bias and resolution for the MCS momentum reconstruction method on this same sample. Here we see that shorter segment lengths tend to have a higher bias. Similarly, shorter segment lengths tend to have better resolution but the difference is small at larger range momenta. For range momenta below about 0.5 GeV the difference in resolution between segment lengths grows because the tracks are short enough that the longer segment lengths are not providing enough sampling points for the MCS method to make an accurate estimation of the track momentum. In order to maintain a gaussian distribution of angular scatters while providing enough sampling points for an momentum resolution of below 10% for the shortest viable tracks, a segment length of 10 cm has been chosen for this analysis.

B Optimizing Constant Detector Resolution Term

This section describes how the resolution term σ_o^{res} in the modified Highland equation, Equation 6 is chosen. The input sample for this study was the high statistics simulated BNB neutrino interactions without any cosmics simulated described in Section 4.1, and this study uses reconstructed tracks that have been selected according to the cuts described in Section 4.4.1. This resolution constant was chosen *after* choosing the optimal segment length of 10 cm described in Appendix A. In order to choose a resolution term, a procedure similar to the one described in the segment length optimization section (Appendix A) is followed. This sample of well-reconstructed truth-selected muons from numu charged current interactions in simulation was analyzed with various different resolution terms. It was found that the resolution term has a very small impact for the muons studied in this sample. It is worth noting that this resolution term will have a stronger impact on the energy resolution the higher energy the muons are (as higher energy muons have smaller angular scatters so the resolution term begins to dominate), but since this study only considers contained muons that have lower energy, the term's impact is weak. It is also worth noting that a muon traversing the entire director would be roughly 10 meters long, which corresponds to a total energy of 2.45 GeV, which corresponds to an RMS scattering angle predicted by Equation 2 σ_o of 4.6 mrad at the start of the track if 10 cm segments are used.

The momentum bias and resolution are computed in the usual way for different resolution terms, using the nominal 10 cm segment length in the algorithm. The results can be seen in Figures 36(a)

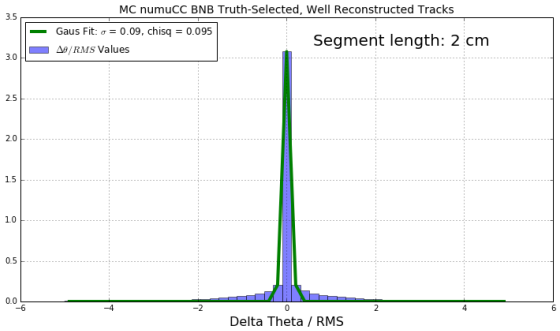

(a) *Highland validation figure for 2 cm segment lengths.*

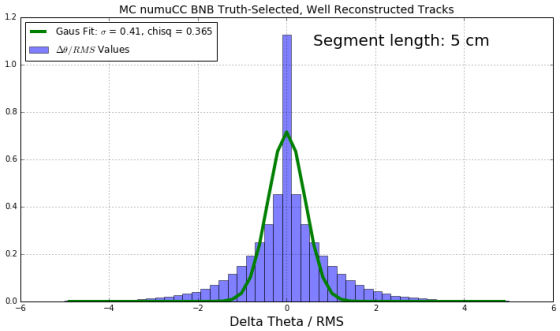

(b) *Highland validation figure for 5 cm segment lengths.*

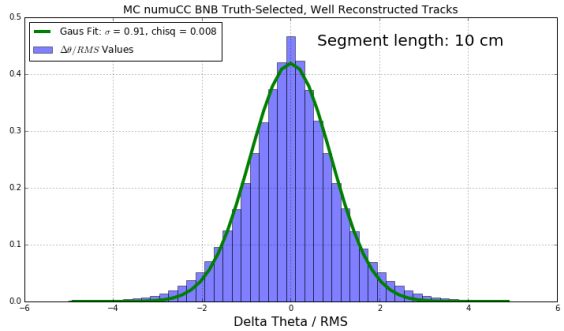

(c) *Highland validation figure for 10 cm segment lengths.*

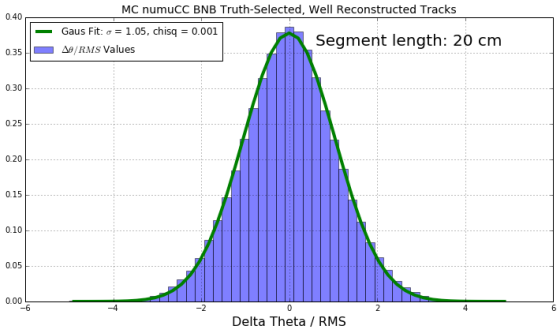

(d) *Highland validation figure for 20 cm segment lengths.*

Figure 34: *Highland validation figures analogous to Figure 14 for various segment lengths, taken from the sample of well reconstructed neutrino-induced truth-selected muons in simulation. The gaussian nature of this plot breaks down for segment lengths that are too short.*

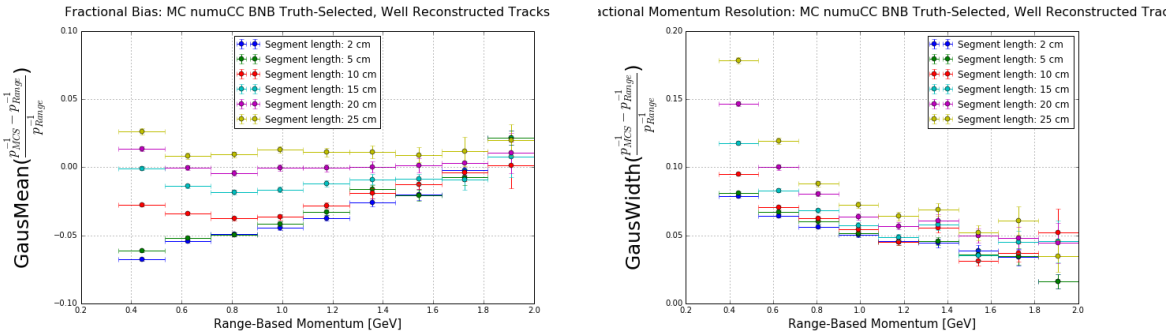

(a) *MCS momentum bias as a function of range momentum for six different segment lengths. The vertical error bars are computed as* $\frac{\sigma_{fit}}{\sqrt{N}}$*, and the horizontal error bars indicate bin width.*

(b) *MCS momentum resolution as a function of range momentum for six different segment lengths. The vertical error bars are computed as* $\frac{\sigma_{fit}}{\sqrt{2N}}$*, and the horizontal error bars indicate bin width.*

Figure 35: *MCS momentum bias and resolution as a function of range momentum for the selected, well reconstructed neutrino-induced truth-selected muons in simulation.*

and 36(b) respectively. Based on the vertical spread between points within each bin in this figure, the resolution terms are shown to have small impact on the bias and momentum resolution of the algorithm so long as the resolution parameter isn't exceedingly large (above 5 mrad) for 10 cm segments. Therefore, a default resolution of 2 mrad has been chosen to be used for the entirety of this analysis.

C MCS to Determine Track Direction

This section demonstrates the ability for the multiple coulomb scattering algorithm to determine the direction of a (fully contained) track. The input sample for this study was the high statistics simulated BNB neutrino interactions without any cosmics simulated described in Section 4.1, and this study uses reconstructed tracks that have been selected according to the cuts described in Section 4.4.1. The MCS code as it is described in Section 3 works by maximizing a likelihood based on angular scatters between segments of a track along with the expected RMS angular deviation from the modified Highland equation (Equation 6). In practice, there is actually a negative log likelihood that is minimized, meaning the lower the likelihood the more confident the fit is. In order to determine the direction of a track with MCS, one can compute the converged minimum negative log likelihood for the track assuming it is oriented in the correct direction, then reverse the ordering of the trajectory points in the track and compute the converged minimum negative log likelihood for the reversed track. The likelihood should be better (smaller) for tracks in the correct direction than their reversed counterparts.

Given this truth-selected sample in simulation, the true direction of the track is known. The minimized negative log likelihood for each of these tracks both in the correct (forwards) direction and incorrect (backwards) direction can be seen in Figure 37(a). A smaller likelihood here means a better fit in the MCS code. Figure 37(b) shows the track-by-track difference of these two distributions, forwards minus backwards. Any negative entries in this figure indicate that the forwards-going track had a better fit

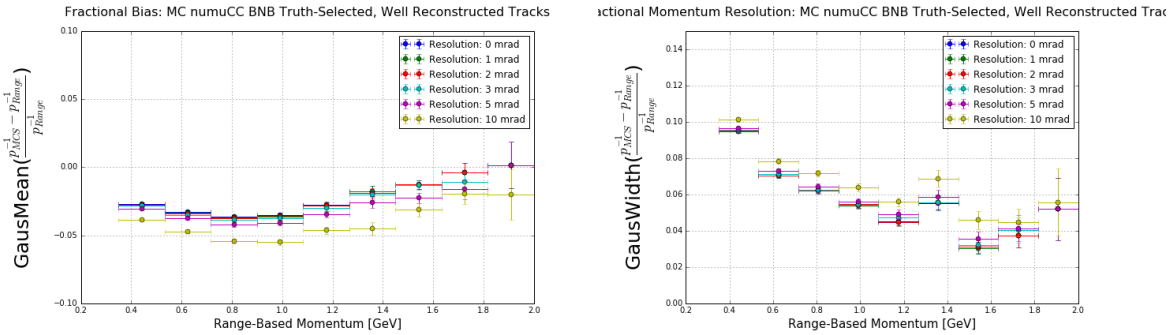

(a) *MCS momentum bias as a function of range momentum for six different resolution terms. The vertical error bars are computed as* $\frac{\sigma_{fit}}{\sqrt{N}}$*, and the horizontal error bars indicate bin width.*

(b) *MCS momentum resolution as a function of range momentum for six different resolution terms. The vertical error bars are computed as* $\frac{\sigma_{fit}}{\sqrt{2N}}$*, and the horizontal error bars indicate bin width.*

Figure 36: *The impact of constant resolution terms,* σ_o^{res} *in the modified Highland equation, Equation 6.*

than backwards-going. This figure shows that MCS can be a powerful tool to test track direction.

D Inverse Momentum to Quantify Resolution: Justification

Throughout this note, the bias and resolution for the MCS momentum estimation method have been computed by fitting gaussians to distributions of $(\frac{p_{MCS}^{-1}-p_{range}^{-1}}{p_{range}^{-1}})$. The Highland formula (Equation 2) predicts gaussian-distributed angular scatters $\Delta\theta$ and is a function of $\frac{1}{p}$. As described by the Opera paper on multiple coulomb scattering[**?**], "since the inverted momentum distribution $\frac{1}{p}$ has a Gaussian shape, the width of the Gaussian divided by $\frac{1}{p_{mean}}$ directly gives the momentum resolution estimate $\frac{\Delta(1/p)}{(1/p)}$."

Purely for visualization sake, to demonstrate that distributions of $(\frac{p_{MCS}^{-1}-p_{range}^{-1}}{p_{range}^{-1}})$ are more gaussian than distributions of $(\frac{p_{MCS}-p_{range}}{p_{range}})$, Figure 38 shows each of these distributions for reconstructed tracks with range energy between 0.35 and 0.53 GeV from the sample of the high statistics simulated BNB neutrino interactions without any cosmics simulated described in Section 4.1.

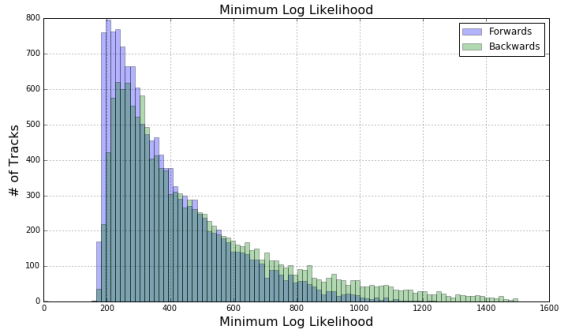

(a) *The minimized negative log likelihood value for each track in the well-reconstructed, fully contained neutrino-induced truth-selected muon tracks in simulation sample, both with tracks oriented in the correct (forwards) direction and reversed (backwards) direction. A smaller likelihood here means a better fit in the MCS code.*

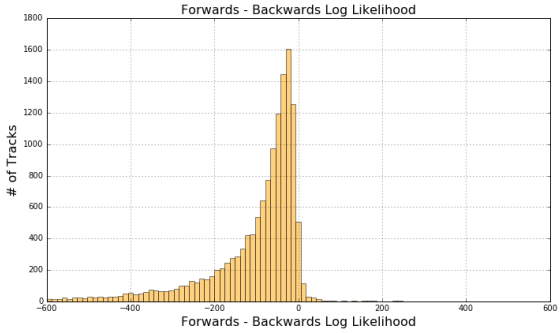

(b) *The track-by-track difference, forwards minus backwards, of the log likelihoods. Negative entries indicate that the forwards-going tracks had a better fit than the backwards-going ones.*

Figure 37: *Evidence that MCS can be used to determine track directions by analyzing the output of the likelihood fit.*

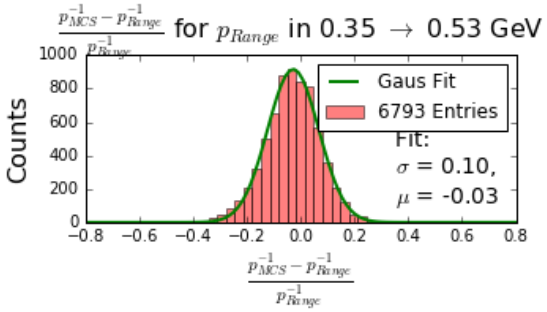

(a) *Fractional momentum difference using inverse momentum, including gaussian fit.*

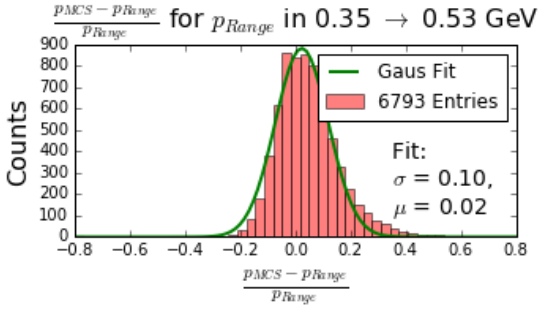

(b) *Fractional momentum difference using normal momentum, including gaussian fit.*

Figure 38: *Fractional momentum differences between 0.35 and 0.53 GeV range energy for well reconstructed muons from the simulated BNB sample with truth-based selection.*

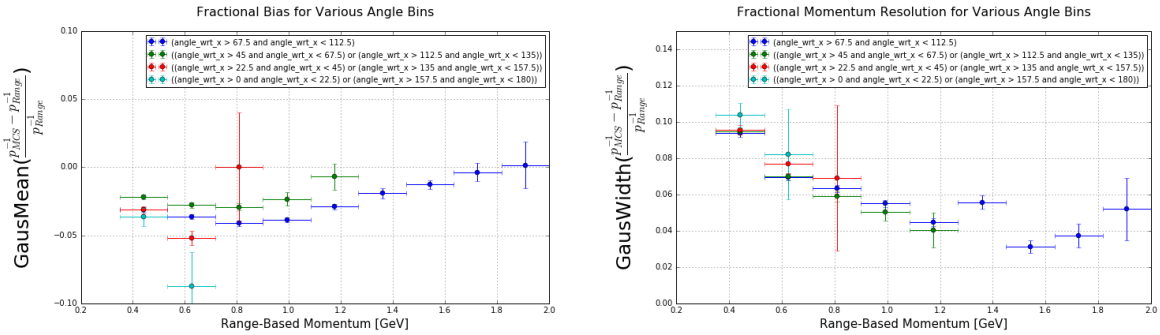

(a) *MCS momentum bias as a function of range-based momentum. The vertical error bars are computed as* $\frac{\sigma_{fit}}{\sqrt{N}}$*, and the horizontal error bars indicate bin width.*

(b) *MCS momentum resolution as a function of range-based momentum. The vertical error bars are computed as* $\frac{\sigma_{fit}}{\sqrt{2N}}$*, and the horizontal error bars indicate bin width.*

Figure 39: *MCS momentum bias and resolution as a function of range momentum for the truth-selected simulated fully contained, well reconstructed muon tracks from numu charged current events. Resolution is broken into four bins of angle with respect to the drift direction: blue are tracks perpendicular to the drift direction to within 22.5 degrees, and cyan are tracks oriented parallel to the drift direction to within 22.5 degrees.*

E Track Angle Dependence

This section describes a brief study of how the performance of the MCS algorithm varies with track angle. The angles of interest are both with respect to the drift direction $x-$, and with respect to the vertical (collection plane wire orientation) direction $y-$. The input sample for this study was the high statistics simulated BNB neutrino interactions without any cosmics simulated described in Section 4.1, and this study uses reconstructed tracks that have been selected according to the cuts described in Section 4.4.1.

The usual bias and resolution plots as a function of range-based momentum for different four bins of angle with respect to the drift direction are shown in Figure 39. Despite limited statistics, it is clear that there is only minimal performance change as a function of angle with respect to the drift direction.

The usual bias and resolution plots as a function of range-based momentum for different four bins of angle with respect to the vertical (collection wire plane orientation) direction are shown in Figure 40. Despite limited statistics, it is clear that there is only minimal performance change as a function of angle with respect to the vertical direction.

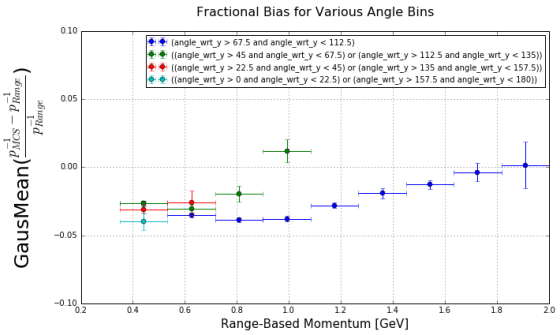

(a) *MCS momentum bias as a function of range-based momentum. The vertical error bars are computed as* $\frac{\sigma_{fit}}{\sqrt{N}}$*, and the horizontal error bars indicate bin width.*

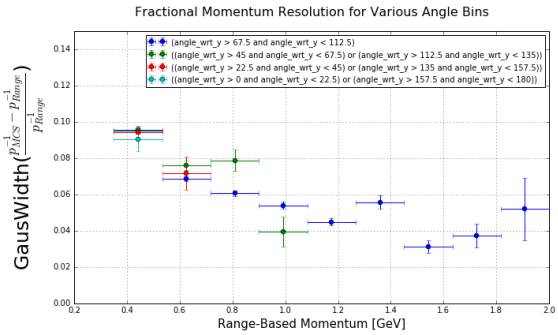

(b) *MCS momentum resolution as a function of range-based momentum. The vertical error bars are computed as* $\frac{\sigma_{fit}}{\sqrt{2N}}$*, and the horizontal error bars indicate bin width.*

Figure 40: *MCS momentum bias and resolution as a function of range momentum for the truth-selected simulated fully contained, well reconstructed muon tracks from numu charged current events. Resolution is broken into four bins of angle with respect to the vertical (collection plane wire orientation) direction: blue are tracks perpendicular to the vertical direction to within 22.5 degrees, and cyan are tracks oriented parallel to the vertical direction to within 22.5 degrees.*

References

[1] A. A. Aguilar-Arevalo *et al.* [MiniBooNE Collaboration], Improved Search for $\bar{\nu}_\mu \to \bar{\nu}_e$ Oscillations in the MiniBooNE Experiment, Phys. Rev. Lett. **110**, 161801 (2013). doi:10.1103/PhysRevLett.110.161801 [arXiv:1207.4809 [hep-ex], arXiv:1303.2588 [hep-ex]].

[2] S. Lockwitz, The MicroBooNE LArTPC, http://www-microboone.fnal.gov/talks/dpfMicroBooNELArTPC.pdf.

[3] V. L. Highland, Some Practical Remarks on Multiple Scattering, Nucl. Instrum. Methods **129** (1975) 104-120.

[4] G. R. Lynch and O. I. Dahl, Nucl. Instrum. Methods Section B (Beam Interactions with Materials and Atoms) **B58, 6** (1991).

[5] K. Kodama *et al.* [DONUT Collaboration], Phys. Lett. B **504**, 218 (2001) doi:10.1016/S0370-2693(01)00307-0 [hep-ex/0012035].

[6] N. Agafonova *et al.* [OPERA Collaboration], New J. Phys. **14**, 013026 (2012) doi:10.1088/1367-2630/14/1/013026 [arXiv:1106.6211 [physics.ins-det]].

[7] G. Giacomelli [MACRO Collaboration], Braz. J. Phys. **33**, 211 (2003) doi:10.1590/S0103-97332003000200008 [hep-ex/0210006].

[8] A. Ankowski *et al.* [ICARUS Collaboration], "Measurement of through-going particle momentum by means of multiple scattering with the ICARUS T600 TPC," Eur. Phys. J. C **48**, 667 (2006) doi:10.1140/epjc/s10052-006-0051-3 [hep-ex/0606006].

[9] L. Kalousis, Momentum measurement via Multiple Coulomb Scattering with the MicroBooNE detector, MicroBooNE Doc-DB-3733.

[10] L. Kalousis, Muon momentum measurement via Multiple Coulomb Scattering in argon, MicroBooNE Doc-DB-4050.

[11] J. S. Marshall and M. A. Thomson, Eur. Phys. J. C **75**, no. 9, 439 (2015) doi:10.1140/epjc/s10052-015-3659-3 [arXiv:1506.05348 [physics.data-an]].

[12] D. E. Groom, N. V. Mokhov and S. Striganov, "Muon Stopping Power and Range Tables: 10 MeV - 100 TeV" Table 5 `http://pdg.lbl.gov/2012/AtomicNuclearProperties/adndt.pdf`

[13] Table 289: Muons in Liquid argon (Ar) `http://pdg.lbl.gov/2012/AtomicNuclearProperties/MUON_ELOSS_TABLES/muonloss_289.pdf`

[14] An et al, Selection of charged-current ν_μ inclusive events - Internal Note, MicroBooNE Doc-DB-5851 `http://microboone-docdb.fnal.gov:8080/cgi-bin/RetrieveFile?docid=5851&filename=cc-incl-neutrino2016-v2.7.pdf&version=9`